3,4-Dihydro-1,3,5-triazin-2(1H)-ones as the First Dual BACE-1/GSK-3β Fragment Hits against Alzheimer's Disease

(Article begins on next page)

27 July 2024

Triazinones as the first dual BACE-1/GSK-3β fragment hits against Alzheimer's disease

Federica Prati,[‡,#] Angela De Simone,[‡,×] Andrea Armirotti,[‡] Maria Summa,[‡] Daniela Pizzirani,[‡] Rita Scarpelli,[‡] Sine Mandrup Bertozzi,[‡] Daniel I. Perez,[⊥] Vincenza Andrisano,[×] Ana Perez-Castillo,[§] Barbara Monti,[#] Francesca Massenzio,[#] Letizia Polito,[∞] Marco Racchi,[ǀ] Piera Sabatino,[ǁ] Giovanni Bottegoni,[‡] Ana Martinez,[⊥] Andrea Cavalli,[*,‡,#] and Maria L. Bolognesi[*,#]

[‡]Department of Drug Discovery and Development, Istituto Italiano di Tecnologia, via Morego 30, 16163 Genova, Italy

[#]Department of Pharmacy and Biotechonology, University of Bologna, via Belmeloro 6/Selmi 3, 40126 Bologna, Italy

[×]Department for Life Quality Studies, University of Bologna, Corso D'Augusto 237, 47921, Rimini, Italy

[⊥]Centro de Investigaciones Biologicas, CIB-CSIC, Ramiro de Maetzu 9, 28040 Madrid, Spain.

[§]Instituto de Investigaciones Biomédicas, CSIC-UAM, Arturo Duperier, 4, 28029 Madrid, Spain and Centro Investigación Biomédica en Red sobre Enfermedades Neurodegenerativas (CIBERNED)

[∞]Fondazione Golgi Cenci, Corso San Martino 10, 20081 Abbiategrasso, Italy

[ǀ]Department of Drug Sciences-Pharmacology, University of Pavia, viale Taramelli 12, 27100 Pavia, Italy

‖Department of Chemistry "Giacomo Ciamician", University of Bologna, via Selmi 2, 40126 Bologna, Italy

ABSTRACT

One of the main obstacles toward the discovery of effective anti-Alzheimer drugs is the multifactorial nature of its etiopathology. Therefore, the use of multitarget-directed ligands has emerged as particularly suitable. Such ligands, able to modulate different neurodegenerative pathways, i.e. amyloid and tau cascades, as well as cognitive and neurogenic functions, are fostered to come. In this respect, we report herein on the first class of BACE-1/GSK-3β dual inhibitors based on a triazinone skeleton, whose hit compound **1** showed interesting properties in a preliminary investigation. Notably, compound **2**, endowed with well-balanced potencies against the two isolated enzymes (IC_{50} of 16 and 7 μM against BACE-1 and GSK-3β, respectively) displayed effective neuroprotective and neurogenic activities and no neurotoxicity in cell-based assays. It also showed good brain permeability in a pharmacokinetic assessment in mice.

Overall, triazinone derivatives, thanks to the simultaneous modulation of multiple points of the diseased network might emerge as suitable candidates to be tested in *in vivo* AD models.

INTRODUCTION

Alzheimer's disease (AD) is the most common form of age-related dementia, and the one with the strongest societal impact for what concerns incidence, prevalence, mortality rate, and cost of care.[1] Against this backdrop, government and industry have increased their support for drug discovery and development. However, despite the past and ongoing massive investments, the available treatments have only moderate palliative effects and a truly disease-modifying drug has yet to come. The cause for the incredible high attrition rate for AD drug discovery has been attributed to several factors, including the fact that the AD pathogenesis is not yet fully understood.[2,3] Nevertheless, what is increasingly recognized is that AD is a multifactorial syndrome,[4] characterized by massive deposits of amyloid-β (Aβ) peptide, neurofibrillary tangles (NTF) of the hyper-phosphorylated τ protein (P-τ), inflammatory mediators, and reactive oxygen species (ROS), leading to neuronal death via a complex array of inter-related pathways.[5] On this basis, only therapeutic tools with a similar complexity and ability to hamper the multiple components of the diseased network might turn effective.[6,7] For this reason, polypharmacological strategies are envisaged as specifically suitable to contrast the complex nature of AD. In this respect, in 2008 we proposed multitarget-directed ligands (MTDLs), namely small organic molecules able to hit multiple targets responsible for the underlying neurodegeneration, as promising therapeutic options.[8] Since then, by appreciating challenges and opportunities, we and others have continued to refine and evaluate multitarget concepts, trying to develop ever better MTDLs against AD.[9-15]

A pivotal aspect for the success of a MTDL drug discovery project is the initial selection of two or more suitable target proteins to start with. In particular, proper targets must not only be validated for AD, but also belong to different neurodegenerative pathways and/or be involved in cognitive and neurogenic functions, thus leading to potential additive or synergistic effects.[16] On

this basis, β-secretase (BACE-1) and glycogen-synthase kinase-3β (GSK-3β) enzymes have emerged as ideal candidates for such multitarget approach. Notably, BACE-1 and GSK-3β belong to the two main pathways of AD that are the amyloid and tau cascade, respectively. Thus, their activities are deeply involved in AD pathogenesis and progression: BACE-1, the aspartyl-protease which catalyzes the cleavage of the amyloid precursor protein (APP),[17] and GSK-3β, the major kinase responsible for τ hyper-phosphorylation,[18] are implicated in the formation of Aβ plaques and NFTs, the two main AD pathological hallmarks.[19, 20] In addition, GSK-3β has been proposed as the possible link between Aβ and τ, and it also modulates inflammatory response, axonal transport and microtubule dynamics impairment, apoptosis, cell cycle deregulation, and adult hyppocampal neurogenesis impairment.[21] Therefore, the simultaneous modulation of both BACE-1 and GSK-3β, by intervening at crucial points in the neurotoxic pathways might represent a breakthrough for the treatment of AD.

On these premises, we have preliminary reported on triazinones as the first class of BACE-1 and GSK-3β dual-inhibitors in the search for innovative disease-modifiers against AD.[22]

In particular, we identified the fluorinated derivative **1** as promising hit fragment with balanced low micromolar activities against the BACE-1/GSK-3β enzymes (Figure 1).[22] In addition, **1** showed an interesting cellular profile in terms of neuroprotection, immunomodulation and neurogenesis, with no sign of toxicity. It also displayed good brain exposure, a fundamental property for central nervous system (CNS)-directed drugs. We also demonstrated that the two enatiomers of **2** displayed a similar enzymatic profile, with no enantioselectivity effect.[22] On this basis and in the pursuit of more effective molecules, we have performed different chemical modifications of the triazinone core, providing compounds **3-34** (Figure 2). Therefore, in this paper, we delineate the general structure-activity relationships (SAR) of **2-34** against BACE-1

and GSK-3β and outline the pharmacological and pharmacokinetic profile of most promising derivatives.

RESULTS AND DISCUSSION

Design. In multitarget drug discovery, fragment-based strategies have been reported to play a pivotal role.[23] Indeed, small fragments, which could be grown by step-wise addition of functional groups, are good starting points for the development of MTDLs. This is based on the assumption that the lower the complexity of a molecule, the higher its probability to interact with multiple biological targets.[24] With these concepts in mind, we exploited a fragment-based approach to design the dual BACE-1/GSK-3β inhibitors **1** and **2**.[22] In particular, we aimed to combine in a single scaffold the pharmacophoric features responsible for binding to BACE-1 and GSK-3β, such as a guanidino motif and a cyclic amide group, respectively (Figure 1). The guanidino moiety, common to several BACE-1 inhibitors, such as acylguanidines and aminoimidazoles may bind to the catalytic aspartic dyad of BACE-1.[25, 26] Whereas, the amino and carbonyl functionalities of the cyclic amide group may act as H-bond donor and acceptor, respectively, thus forming H-bond interactions with the backbone of GSK-3β hinge region. This cyclic amide function, present in numerous ATP-competitive inhibitors of GSK-3β, that is indirubines, maleimides, and paullones, among others, seems to play a key role in the kinase binding, providing a specific H-bond network.[27]

As a result, the 6-amino-4-phenyl triazinone scaffold was identified by means of molecular modelling studies as potential starting point with the aforementioned structural features (Figure 1). On this basis, a preliminary SAR exploration of the triazinone core with respect to the substituent on the *para*-position of the phenyl ring (F, CF$_3$, Br, CH$_3$, N(CH$_3$)$_2$), led to the 4-fluoro derivative **1**.[22] With **1** in hand, herein we have expanded the aromatic substitution pattern,

and a new set of twenty five 6-amino triazinones (**3-27**, Figure 2) was developed. In particular, various electron-withdrawing and electron-donating groups at the *ortho* (*o*), *meta* (*m*) and *para* (*p*) positions of the phenyl ring, as well as the replacement with other heteroaromatic nuclei were investigated. The substituents were selected for both SAR and solubility purposes. Notably, to cover this latter aspect, compounds **18-21**, bearing a polar group on the aromatic ring, such as diethylamino, morpholino, piperidino, and 4-methyl-piperazino functions, were synthesized. These solubilizing moieties were carefully selected among those structural elements more frequently employed for the design or optimization of a CNS drug.[28]

Afterwards, we planned the isosteric replacement of the 3,4-dihydro-triazinone carbonyl oxygen with a sulphur atom, to access a subset of 3,4-dihydro-triazinthiones **28-31** (Figure 2).

In addition, on the basis of the well-balanced activities of the 6-ethylamino derivative **2** against both targets, the introduction of different *N*-alkyl and *N*-aryl groups on the exocyclic amino group at position C6 was also envisaged, providing derivatives **32-34** (Figure 2).

Considering the lack of stereorecognition by the target enzymes of enantiomers (-)-**2** and (+)-**2**,[22] all compounds were synthesized and tested as racemates.

Chemistry. Compounds **3-27** were synthesized following the two-step synthetic route optimized for the synthesis of **1**[22] (Scheme 1). First, the acid-catalyzed hydration of 1-cyanoguanidine **35** provided guanylurea sulfate **36** in excellent yield. Subsequently, **36** was coupled to the aromatic aldehydes of interest (**37-61**) through a condensation reaction,[29] affording the target compounds **3-27** in poor to moderate yields (10-71%).

All the aromatic aldehydes used in the cyclization were purchased from commercial vendors, with the exception of 4-(aminomethyl)benzaldehydes **52-55**. These were prepared following a reported three step-synthetic protocol,[30] slightly modified (Scheme 2). The commercially

available methyl 4-(bromomethyl)benzoate (**62**) underwent nucleophilic substitution with the suitable amines **63-66** to provide methyl 4-(aminomethyl)benzoates **67-70**. Subsequent reduction with $LiAlH_4$ provided the corresponding alcohols **71-74**, which were then oxidized under Swern conditions to afford aldehydes **52-55** in good yield. Notably, this synthetic pathway resulted more efficient with respect to the attempted single-step reduction of **67** to **52** by lithium bis(diethylamino)aluminum hydride (not shown).

6-Amino-4-aryl-3,4-dihydro-1,3,5-triazinthiones **28-31** were synthesized by treatment of the commercially available 2-imino-4-thiobiuret **75** with benzaldehydes **76**, **42**, **77**, and **49**, according to the aforementioned cyclization procedure (Scheme 3).

6-alkyl/arylamino-4-aryl-3,4-dihydro-1,3,5-triazin-2(1*H*)-ones **32-34** were prepared following the two-step synthetic route described for **3-27**. However, in this case an additional step was necessary to provide the starting alkylcyanoguanidines **78-80** (Scheme 4). To this end, the commercially available sodium dicyanamide **81** was treated with the amines of interest **82-84** to afford the corresponding **78-80**. These were then converted to alkylguanylurea derivatives **85-87** by the developed acid-catalyzed hydration and then coupled with the aldehyde of interest **49** and **77** in concentrated H_2SO_4, providing **32-34**.

X-ray structure of 2. Concerning the possibility of different tautomeric forms, that could generate different H-bonding patterns, single crystal X-ray investigations on **2** were performed. They unambiguously showed that two independent molecules (A and B) are present in the asymmetric unit, plus a water molecule (crystallization medium) strictly connected to both of them. The molecular and crystal structure of **2** (CCDC 0001000228543) is shown in Figure 3 together with its crystallographic numbering and main geometrical parameters. Molecule B shows the expected endocyclic double bond at N(1)-C(9), 1.28(1) Å, with C(9)-N(4) 1.35(1) Å in

length, while molecule A presents almost equivalent bond lengths for the corresponding atom pairs. This feature is kept even at low temperature: a new data collection at T = 100 K confirmed the same molecular distribution in bond lengths, allowing to infer that, while one independent molecule shows an endocyclic N-C double bond, the two *endo-* and *exo-* tautomers equally contribute for the second molecule in the asymmetric unit. Also, due to different spatial orientations of phenyl rings, two conformers for each phenyl rings are present in the solid state. Moreover, the flexibility in C_2H_5-NH side chain bound to C(9) gives rise to two different conformational isomers in the A-B pair: fully extended in B (torsion angle 173.5°) while exhibiting a *gauche* conformation in A (torsion angle 114° ca).

At a supramolecular level, a strong network of hydrogen bonding involving the water molecule connects A and B molecules according to the following scheme: O_water...N(1A), O_water…N(1B), and O_water...O(1A) (data not shown).

A and B molecules display a sort of anti-parallel orientation of the HN-triazinone moieties which allows to form further strong H-bonds, shorter than 3.0 Å, between O(1A), N(2A) and N(4A) and their N(4B), N(2B) and O(1B) counterparts, contributing to the "hetero" tautomers recognition. Aromatic interactions between phenyl rings further contribute to the supramolecular assembly (data not shown).

The presence of different conformers in the same crystal is linked to the low energy difference among the different forms.[31] However, it is known that even a slightly disfavored torsional geometry may be compensated by a better H-bonding or aromatic interaction. Molecular conformation and hydrogen bonding (or π-π stacking interactions) can thus influence each other and, in turn, the overall crystal packing.

The possibility of different conformers and tautomeric forms lands support to the high molecular versatility of the triazinone fragment and to its potential as a multitarget ligand.[23, 32]

Biological evaluation. We have envisaged MTDLs as the most powerful options for the treatment of AD, a multifactorial syndrome that currently available single-target drugs cannot cure. The MTDLs developed herein were rationally designed to hit two main AD-related targets, that is BACE-1 and GSK-3β enzymes. Thus, by intervening at two crucial points of the amyloid and tau network, they may display a truly disease-modifying effect against AD. To this end, very recently Aβ and tau anti-aggregating agents[33] and dual inhibitors of the tau kinase Dyrk 1A and of Aβ aggregation[34] have been reported.

To disclose the proposed dual-target profile for the newly synthesized compounds, a number of assays were performed, including BACE-1 and GSK-3β inhibition in biochemical assays, as well as the cellular neuroprotective and neurogenic effects mediated by the inhibition of the two enzymes. Furthermore, brain permeation was preliminary assessed *in vitro* in parallel artificial membrane permeability assay (PAMPA-BBB), and *in vivo*.

Enzymatic profile. As a primary screening, the ability of compounds **3-34** to inhibit both BACE-1 and GSK-3β activities was investigated in comparison to inhibitor IV and SB415286 as reference compounds for BACE-1 and GSK-3β, respectively, as well as the parent compounds **1** and **2**. The anti-β-secretase potential of **3-34**, was determined in a biochemical assay based on the cleavage of a peptide substrate mimicking the human APP sequence with the Swedish mutation (methoxycoumarin-Ser-Glu-Val-Asn-Leu-Asp-Ala-Glu-Phe-Lys-dinitrophenyl), using the fluorescence resonance energy transfer (FRET) methodology.[35] GSK-3β biochemical inhibition was assessed using the Kinase-Glo luminescent assay, which quantifies the decrease in

ATP levels following the kinase reaction.[36] IC$_{50}$ values on the two enzymes are reported in Table 1, and were determined by using the linear regression parameters.

Considering the 6-amino-4-aryl-triazinone series (**3-27**), all tested compounds modulated GSK-3β activity in the double-digit micromolar range (10.14 μM ≤ IC$_{50}$ ≥ 57.65 μM), with the exception of 4-((diethylamino)methyl)phenyl (**18**) and 4-((*N*-methylpiperazino)methyl)phenyl (**21**) derivatives, which resulted less effective GSK-3β inhibitors (IC$_{50}$ > 100 μM). These results indicate that no significant improvement in GSK-3β inhibitory activity was achieved with this new series of compounds, with derivatives **8** (2-F), **15** (2-CH$_3$) and **23** (3,4-diCl) being equipotent to hits **1** and **2**.

With regards to BACE-1, the 6-amino-4-(*o*-, *m*-, *p*-halogen)-substituted triazinones **6-14**, the 3,4-dichloro- and 3,5-difluoro-substituted derivatives **23** and **24**, and the 3-pyridinyl analogue **26** showed interesting IC$_{50}$ values, ranging from 10.18 to 84.72 μM. The promising anti-β-secretase activity of the halogenated **6-14**, **23**, and **24** could likely derive from the possibility for the halogen atoms to establish polar and hydrophobic interactions at specific enzymatic subsites, such as a cage made by Leu30, Ile118, Phe108, and Trp115 at subsite P1. Notably, the 3-F-phenyl derivative **9** resulted the most active β-secretase inhibitor, with an IC$_{50}$ of 10.18 ± 1.02 μM, which is even slightly improved with respect to the 4-F-phenyl derivative **2**.

Generally, triazinthiones **28-30** were active in the micromolar range against both enzymes (13.78 μM ≤ IC$_{50}$ ≥ 39.00 μM for GSK-3β; 43.15 μM ≤ IC$_{50}$ ≥ 60.19 μM for BACE-1) and showed similar or higher activities compared to the corresponding triazinones. Therefore, the oxygen/sulfur isosteric replacement at position 2 of the triazinone core only marginally affected activity.

N-alkyl/*N*-aryl derivatives **32-34** displayed low micromolar activities against GSK-3β (4.34 μM ≤ IC$_{50}$ ≥ 40.71 μM). Remarkably, **33** and **34** together with the parent compound **2** showed IC$_{50}$ values in the single-digit micromolar range, with the propyl derivative **33** as the most potent GSK-3β inhibitor of the whole series (IC$_{50}$ = 4.34 μM). As for BACE-1, **32** and **33** turned out to be moderate inhibitors, with IC$_{50}$ ranging from 36 to 50 μM, whereas **34** did not show any significant effect up to a concentration of 100 μM. It can be derived that alkylation and arylation of the 6-amino group of the triazinone core slightly improve the anti-GSK-3β potency, probably due to the generation of weak hydrophobic interactions within the binding pocket of the enzyme. Conversely, the introduction of the same substituents, especially the aryl moiety of **34**, negatively affects BACE-1 inhibitory activity. This is likely due to the fact that these substituents generate steric and electronic effects that might hamper BACE-1 aspartyl dyad recognition.

Overall, the collected SAR results revealed that, despite the number of synthesized congeners, the parent compounds **1** and **2** are still the most promising from a multitarget standpoint, with a balanced enzymatic profile and good ligand efficiency (LE) metrics against the two targets.[22] In particular, LE metrics, that is measures of the *in vitro* biological activity corrected for the physicochemical property 'load' of a molecule, account for the effective use of the molecule's structural features in binding to the target.[37] In this respect, LE metrics has recently found increasing application in fragment-based drug discovery as useful tool to normalize the low binding affinities (1 mM to 10 μM) of fragment hits and to identify and prioritize the best starting points for a subsequent fragment-to-lead campaign.[37] Therefore, despite the moderate activity, we have proposed that **1** and **2**, due to their structural simplicity, low molecular weight, and favorable LE values, might be suitable binder.

On this basis, **2** was pursued for further cellular studies. Moreover, derivatives **9** and **33**, being the most active BACE-1 and GSK-3β inhibitors of the series, respectively, were also selected for additional investigations.

Aβ(1-40) secretion. The effect of **9** and **33** on the secretion of Aβ(1-40) was examined in cellular context, in comparison with parent compounds **1**[22] and **2**[22]. The anti-β-secretase activity of the tested compounds in neuroglioma cell line overexpressing the *h*APP gene harboring the KM670/671NL (Swedish) mutation (H4-APP$_{sw}$) is reported in Figure 4a. H4-APP$_{sw}$ cells were treated with **1**, **2**, **9**, and **33** for 24 h at a concentration corresponding to their respective IC$_{50}$ values on BACE-1. Similarly to what observed for **1** and **2**, in the case of **9** enzymatic activity was mirrored by a moderate reduction of cellular Aβ levels, though with much less effectiveness with respect to the reference inhibitor (inhibitor IV). As regards to **33**, which is the poorest BACE-1 inhibitor among the selected ones, the observed activity is negligible. As a positive feature, Figure 4b shows that **1**, **2**, **9**, and **33** did not affect H4-APP$_{sw}$ cell viability at the tested concentrations, as monitored through the colorimetric tetrazolium salt (MTT) assay. So, a low neurotoxicity for the triazinone chemotype may be anticipated.

Neuroprotection. The effects of **2**, **9**, and **33** on neuroprotection were also assessed, in comparison with **1**.[22] In fact, neuroprotection, preserving neuronal structure and functionality against toxic insults, and thus reducing neuronal loss and degeneration, is a crucial property for new AD-modifying drugs.

Various pro-inflammatory stimuli might enhance GSK-3β activity, resulting in increased level of glia activation and in a peculiar cytokines pattern, ultimately leading to the neuronal cell death in AD.[38] Therefore, we explored the potential neuroprotective activity of the selected compounds in primary cultures of astrocytes and microglia, by evaluating nitrite production.

As reported for **1**,[22] primary cultured glial cells were first incubated with compounds **2**, **9**, and **33** (10 μM) for 1 h, and then cultured for further 24 h with lipopolysaccharide (LPS) (10 μg/mL), a potent cytotoxic inducer of inflammation and of a cascade of intracellular events involved in neuronal death. In LPS-treated cells, we observed an important induction of nitrite production, which was significantly reduced by treatment with **2** and **33** (Figure 5). Their observed cellular activities nicely match their inhibitory potencies on GSK-3β isolated enzyme. Indeed, **2** and **33,** displaying enzymatic potency in the single-digit micromolar range, turned out to be potent neuroprotective agents at 10 μM concentration. To note, **2** and **33** were mostly effective on astrocytes, where they significantly drop nitrite production to levels lower than the basal ones. On the other hand, **9**, with an IC_{50} of 32.41 μM against GSK-3β, showed modest activity on microglia, but no effect on astrocytes, where it even caused an increase in nitrite generation.

Importantly, similar results were also obtained by co-treatment of primary rat glial cells with LPS and compounds **2** and **33** at different concentrations (0, 5, 10, 20 and 50 μM) (Figure S1). Motivated by these interesting findings, we investigated the observed neuroprotective activities of **2** and **33** more in depth. In particular, we evaluated the ability of our compounds to modulate the glial phenotypic switch from the pro-inflammatory M1 to the anti-inflammatory M2 type. Importantly, the transformation from the neuroprotective M2 to the cytotoxic M1 glial cells is now considered a crucial step in the progression of neurodegenerative diseases, including AD.[39] Therefore, compounds that prompt the switch from the M1 to M2 form have been proposed as capable to attenuate neuroinflammation and boost neuronal protection and recovery. In details, this M1/M2 phenotypic classification is based on a specific pattern of pro- or anti-inflammatory cytokines and receptors, whose release and expression is regulated, among others, by GSK-3β activity.[40] In this respect, GSK-3β activation has been reported to foster and maintain the pro-

inflammatory state. On this basis, we evaluated the ability of **2** and **33** to modulate the expression level of the inducible nitric oxide synthase (iNOS) as M1 marker, and the triggering receptor expressed on myeloid cells 2 (TREM2) as M2 marker on glial cells. iNOS, an inducible enzyme with a prevailingly glial localization, is expressed upon pro-inflammatory stimulation and it is responsible for the elevated NO concentrations associated with the neurodegenerative pathology,[41] whereas TREM2 stimulates phagocytosis for Aβ clearance and suppresses cytokine release, thus reducing inflammation.[42]

We were pleased to verify that when cultures of primary rat glial cells were stimulated with LPS, we observed the expected iNOS induction, which was reduced by a 24 h co-treatment with **2** and **33** in a dose-dependent manner and to a greater extent than what reported for **1** (Figures 6a-d). Furthermore, along the same line, in microglia cells treated with LPS we observed a reduction of TREM2 expression, which was restored by 24 h co-treatment with **2** and **33** (Figures 6d and e). Altogether these results indicate that **2** and **33** are highly promising anti-inflammatory and neuroprotective agents, able to decrease the neurotoxic microglial activation, while not affecting the neuroprotective one. Moreover, **2** and **33** did not display any toxicity in glial and neuronal cells up to 50 μM (Figure S2).

Neurogenesis. Neurogenesis is a crucial property for new AD-modifying drugs, since it confers the potential to increase endogenous regeneration as a repair mechanism in the damaged brain, and reduce neuronal loss and degeneration. In this respect, considering that GSK-3β inhibition has been reported to regulate and increase neurogenesis,[43, 44] we verified whether addition of **2**, **9**, and **33** to neurosphere (NS) cultures of primary rat neural stem cells could regulate cell differentiation toward a neuronal phenotype. The NSs were cultivated in the absence or presence of compounds **2**, **9**, and **33** (10 μM) during a week. After that, they were first incubated with

anti-β-tubulin and anti-microtubule associated protein 2 (MAP-2) antibodies, and then treated with the corresponding labelled secondary antibodies to reveal the immature and mature neuronal markers β-tubulin (green label) and MAP-2 (red label), respectively. Encouragingly, evident neurogenic effects were detected after treatment of NSs with **2** and **33** (Figure 7). Particularly, when compared to control and even to parent compound **1**, the number of β-tubulin positive cells was considerately augmented in cultures treated with **2**, whereas, **33** significantly amplified the number of MAP-2 positive cells. Moreover, **2** and **33** showed a dense crown of either β-tubulin or MAP-2-positive cells around the NS core and additional positive cells outside of it, suggesting a migration out of the NS.

Notably, these findings underlined the ability of **2** and **33** to differentiate neural stem cells to immature and mature neurons, respectively. Furthermore, our results also demonstrate that **2** and **33** can induce migration of cells out of the NSs. These outcomes are particularly relevant in a clinical setting, since the identification of small molecules that not only promote neural stem cell differentiation as endogenous regenerative and repair mechanisms, but also affect their migration capacity might have an important regulatory role in hippocampal migratory events in a brain injury context.[44]

Blood-brain-barrier (BBB) penetration. The BBB penetration has been considered as a major bottleneck in CNS drug development and as an important factor limiting the future growth of neurotherapeutics.[45] Therefore, to reduce attrition rate, the brain permeability of new CNS-directed molecules needs to be evaluated in the early drug discovery stage. Considering that the majority of CNS drugs enter the brain by transcellular passive diffusion, PAMPA-BBB has been proposed as a useful high throughput technique to predict passive permeability through biological membranes.[46] Hence, prediction of brain penetration for compounds **1-34** was

evaluated in PAMPA-BBB, using a brain lipid porcine membrane. First, an assay validation study was carried out by testing ten commercial drugs and comparing the obtained permeability (*Pe*) values with the corresponding literature data. A good linear correlation between the two data set was obtained: $Y_{experimental} = 1.1999X_{literature} - 0.8494$ ($R^2 = 0.974$) (Figure S3). According to this equation and following the pattern established in the literature for BBB permeation prediction,[47] we could classify compounds as able to enter the brain when they present $Pe > 3.95 \times 10^{-6}$ cm s^{-1}. Unfortunately, all our compounds, but **22** and **34**, showed low *Pe* and were predicted not to penetrate the CNS (Table S1). However, considering that **1** showed an interesting *in vivo* pharmacokinetic profile,[22] and that triazinones are small and polar molecules, we reasoned that the PAMPA-BBB model is not the right one for the current series. Indeed, it is highly conceivable that they do not cross BBB by passive diffusion, but rather might exploit membrane specific transporters to enter the brain, i.e. the guanidine compound trasporters.[48] Accordingly, we generated mouse pharmacokinetic data for compound **2**. Notably, **2** showed good BBB penetration, confirming that triazinones may rely on different mechanisms rather than passive diffusion to enter the brain.

In details, 15 min after intraperitoneal dosing of **2** (10 mg kg^{-1}), we measured a maximal plasma concentration of 695 ng mL^{-1}, accompanied with an half-life for the elimination phase of 163 min. **2** showed a volume of distribution of 7.2 L kg^{-1} and disappeared from the systemic circulation with a clearance of 306 mL min kg^{-1}. Importantly, **2** reached a maximum concentration in 1 mL of brain homogenate of 1.50 ng/mg$_{protein}$, 30 min after administration (Table 2). On this basis we could approximately estimate that **2** reached total cerebral levels of 1.34 μM, which, although not ensuring *in vivo* target engagement, represent a promising starting point towards an efficacious hit optimization campaign (details of the calculation are reported in

the Experimental Section). Indeed, effective *in vivo* concentrations could be reached by lowering IC_{50} values on both enzymes just around 10 folds or even less, considering that a peritoneal administration of 10 mg kg^{-1} dose is not very high, and it can be increased.

CONCLUSIONS

Herein, we described a new series of derivatives belonging to the first class of dual inhibitors of BACE-1/GSK-3β enzymes, two of the most validated targets in AD drug discovery. The remarkable neuroprotective and neuroregenerative profile shown by **2** is undoubtedly the most promising achievement of the current investigation, and support the idea that balanced, although relatively low inhibitory potencies are key molecular features for such dual inhibitors.

This is reinforced by the suggestion that a partial inhibition of BACE-1 and GSK-3β might provide clinical benefits with limited side effects. Heterozygous BACE-1 knockout APP transgenic mice with an only 15% reduction in Aβ cerebral level showed a significant reduction in brain amyloid burden at old age.[49] As for GSK-3β, considering that it is generally up-regulated in neurodegenerative conditions, a similar mild inhibition would be enough to produce an important therapeutic effect.[50] Particularly, a smooth inhibition of GSK-3β would normalize its activity in the diseased tissues, without significantly affecting the healthy ones, where compensatory mechanisms will likely balance the deficit.[51]

More importantly, a basic concept of polypharmacology is that where connections exist between two targets within a network, dual inhibitors with only moderate activities produce superior *in vivo* effects compared to higher-affinity single-targeted compounds, and with potential minor toxicity.[32, 52]

Indeed, a cross-talk between the BACE-1 and GSK-3β has been clearly demonstrated. BACE-1 fosters Aβ generation, which exerts its neurotoxic effects in a variety of ways. Particularly, Aβ has been reported to induce GSK-3β activation,[53] thus increasing τ-phosphorylation and NFT toxicity, neuroinflammation, apoptosis, cell cycle deregulation, and impairment of adult hippocampal neurogenesis. What's the more, GSK-3β not only responds to Aβ peptide, but it also regulates its accumulation, by modulating α-, β- and γ-secretase enzymatic activities,[54-56] thus establishing a vicious feed-forward loop.

In addition, the conformational flexibility of **2** highlighted by the crystal structure elucidation expands the multitarget potential of this fragment.

Therefore, we are confident that triazinone derivatives, thanks to the simultaneous, moderate modulation of multiple points of the inextricably intertwined pathways leading to amyloid and tau, a low toxicity and a favourable BBB permeation, might emerge as suitable candidates to be tested in *in vivo* model of AD.

METHODS

Chemistry. All the commercial available reagents and solvents were used as purchased from Sigma-Aldrich, Fluka (Italy) and Alfa Aesar (Germany) without further purification.

Column chromatography purifications were performed under "flash conditions" using Sigma-Aldrich silica gel grade 9385, 60 Å, 230−400 mesh. Thin layer chromatography (TLC) separations were performed on 0.20 mm silica gel 60 F254 plates (Merck, Germany), which were visualized by exposure to ultraviolet light (254 and 366 nm), and potassium permanganate stain. Reactions involving generation or consumption of amine were visualized by using bromocresol green spray (0.04% in EtOH made blue by NaOH) following heating of the plate.

Compounds were named following IUPAC rules as applied by ChemBioDraw Ultra (version 13.0).

The purifications by preparative high performance liquid chromatography-mass spectrometry (HPLC/MS) were run on a Waters Autopurification system consisting of a 3100 single quadropole mass spectrometer (SQD-MS) equipped with an electrospray ionization (ESI) interface and a 2998 photodiode array detector (PDA). The HPLC system included a 2747 sample manager, 2545 binary gradient module, system fluidic organizer and 515 HPLC pump. The separations were performed on a XBridge^{TM} prep C_{18} OBD column (100 × 19 mm ID, particle size 5 µm) with a XBridge^{TM} prep C_{18} (10 × 19 mm ID, particle size 5µm) guard cartridge, using 10 mM NH_4OAc in H_2O at pH 5 adjusted with AcOH (A) and 10 mM NH_4OAc in MeCN-H_2O (95:5) at pH 5 (B) as mobile phase. A linear gradient was applied starting at 0% B (initial hold for 0.5 min) to 40% B in 7 min. From 40% to 100% B in 0.1 min and hold at 100% for 2.4 min. The PDA range was 210-400 nm. ESI in positive mode was used in the mass scan range 100-500 Da.

Nuclear magnetic resonance (NMR) experiments were run on Varian VXR 200 and 400 and Bruker Avance III 400 (200 and 400 MHz for ^{1}H; 50 and 100 MHz for ^{13}C). Spectra were acquired at 300 K, using DMSO-d_6, CD_3OD, D_2O and $CDCl_3$ as solvents. Chemical shifts for ^{1}H and ^{13}C spectra were recorded in parts per million (ppm) using the residual non-deuterated solvent as the internal standard (I.S). Data are reported as follows: chemical shift (ppm), multiplicity (indicated as: s, singlet; br s, broad singlet; exch, exchangeable proton with D_2O; d, doublet; t, triplet; q, quartet; m, multiplet and combinations thereof), coupling constants (*J*) in Hertz (Hz) and integrated intensity.

Ultra performance liquid chromatography-mass (UPLC-MS) analyses were run on a Waters ACQUITY UPLC-MS system consisting of SQD-MS equipped with an ESI interface and a PDA detector. PDA range was 210-400 nm. Analyses were performed on an ACQUITY UPLC HSS T3 C_{18} column (50 mm × 2.1 mm ID, particle size 1.8 μm) with a VanGuard HSS T3 C_{18} precolumn (5 mm × 2.1 mm ID, particle size 1.8 μm). Mobile phase was 10 mM NH_4OAc in H_2O at pH 5 adjusted with AcOH (A) and 10 mM NH_4OAc in MeCN-H_2O (95:5) at pH 5 (B). ESI in positive and negative mode was applied, in the mass scan range 100-500 Da.

Melting points were determined in glass capillary tubes on a Gallenkamp melting point apparatus and are uncorrected.

All the finals compounds showed ≥95% purity by NMR and UPLC-MS (UV at 215nm) analysis.

General procedure (A) for the synthesis of methyl 4-((amino)methyl)benzoates (67-70). To an ice-cold solution of methyl 4-(bromomethyl)benzoate **62** (1.0 eq.) in THF (0.7 M), the proper amine (**63-66**) (4.0 eq.) was added. The reaction mixture was heated at 100 °C under microwave irradiation for 20 min, affording a white precipitate, which was filtered off. The filtrate was concentrated under vacuum, and the resulting residue was taken up with 30 mL of 2N aqueous HCl solution. The aqueous phase was washed with Et_2O (30 mL × 3), made basic with Na_2CO_3, and extracted with EtOAc (30 mL × 3). The organic layers were collected, dried over anhydrous Na_2SO_4, filtered, and concentrated under vacuum. The so obtained title compound (**67-70**) was used in the next step without further purification.

Methyl 4-((diethylamino)methyl)benzoate (67). The title compound was synthesized according to general procedure A using diethylamine **63** (2.4 g, 35.00 mmol). **67** was obtained as a yellow

oil: 1.73 g (90%). ^{1}H-NMR (CDCl$_3$, 400 MHz) δ 1.03 (t, J = 7.2 Hz, 6H), 2.51 (q, J = 7.2 Hz, 4H), 3.60 (s, 2H), 3.89 (s, 3H), 7.41 (d, J = 8.4 Hz, 2H), 7.97 (d, J = 8.4 Hz, 2H). ^{13}C-NMR (CDCl$_3$, 100 MHz) δ 11.8, 46.9, 51.8, 57.4, 128.4, 128.5, 129.4, 145.8, 167.0

Methyl 4-(morpholinomethyl)benzoate (68). The title compound was synthesized according to general procedure A using morpholine **64** (3.0 g, 35.00 mmol). **68** was obtained as a yellow oil: 1.80 g (90%). ^{1}H-NMR (CDCl$_3$, 400 MHz) δ 2.24-2.25 (m, 4H), 3.33 (s, 2H), 3.50-3.52 (m, 4H), 3.71 (s, 3H), 7.22 (d, J = 8.4 Hz, 2H), 7.81 (d, J = 8.4 Hz, 2H).

Methyl 4-(piperidin-1-ylmethyl)benzoate (69). The title compound was synthesized according to general procedure A using piperidine **65** (2.98 g, 35.00 mmol). **69** was obtained as a yellow oil: 1.89 g (94%). ^{1}H-NMR (CDCl$_3$, 400 MHz) δ 1.37-1.42 (m, 2H), 1.50-1.55 (m, 4H), 2.31-2.33 (m, 4H), 3.46 (s, 2H), 3.86 (s, 3H), 7.35 (d, J = 8.4 Hz, 2H), 7.93 (d, J = 8.4 Hz, 2H).

Methyl 4-((4-methylpiperazin-1-yl)methyl)benzoate (70). The title compound was synthesized according to general procedure A using *N*-methylpiperazine **66** (3.50 g, 35.00 mmol). **70** was obtained as a yellow oil: 2.10 g (97%). ^{1}H-NMR (CDCl$_3$, 200 MHz) δ 2.21 (s, 3H), 2.38-2.42 (m, 8H), 3.50 (s, 2H), 3.84 (s, 3H), 7.34 (d, J = 8.4 Hz, 2H), 7.94 (d, J = 8.4 Hz, 2H).

General procedure (B) for the synthesis of methyl 4-((amino)methyl)benzyl alchools (71-74). To an ice-cold suspension of LiAlH$_4$ (2.0 eq.) in anhydrous THF (2.3 M), a solution of methyl 4-((amino)methyl)benzoate (**67-70**) (1.0 eq.) in the same solvent (1.6 M) was added dropwise. After stirring at rt for 2 h, the reaction mixture was cooled down in an ice-bath, and

quenched by slow addition of cold water (4 mL). The resulting mixture was stirred at 0 °C for 30

min, added to 1N aqueous NaOH solution (4 mL) and stirred at 0 °C for additional 10 min. This

suspension was diluted with Et_2O and filtered through a Celite cake. The filtrate was

concentrated *in vacuo*, and the resulting residue was taken up with EtOAc (20 mL) and washed

with H_2O (20 mL). The organic phase was dried over anhydrous Na_2SO_4, filtered and

concentrated under vacuum to afford the title compound (**71-74**). Further purification by flash

chromatography was performed when required.

(4-((Diethylamino)methyl)phenyl)methanol (71). The title compound was synthesized from **67**

(1.10 g, 5.00 mmol) according to general procedure B. **71** was obtained as a yellow oil: 0.84 g

(88%). ^{1}H-NMR (CDCl_3, 400 MHz) δ 0.99-1.03 (m, 6H), 2.45-2.50 (m, 4H), 3.52 (s, 2H), 4.55

(s, 2H), 7.24-7.26 (m, 4H). ^{13}C-NMR (CDCl_3, 100 MHz) δ 11.4, 46.4, 56.0, 64.5, 126.8, 129.2,

138.0, 140.0.

(4-(Morpholinomethyl)phenyl)methanol (72). The title compound was synthesized from **68**

(1.80 g, 7.65 mmol) according to general procedure B. Elution with DCM/MeOH/33% aqueous

NH_3 solution (9:1:0.1) afforded **72** as light pink solid: 1.40 g (88%). ^{1}H-NMR (CDCl_3, 400

MHz) δ 2.30-2.32 (m, 4H), 3.38 (s, 2H), 3.55-3.57 (m, 4H), 4.00 (br s, exch, 1H), 4.51 (s, 2H),

7.18-7.22 (m, 4H). ^{13}C-NMR (CDCl_3, 100 MHz) δ 53.4, 63.0, 64.3, 66.7, 126.9, 129.4, 136.3,

140.4.

(4-(Piperidin-1-ylmethyl)phenyl)methanol (73). The title compound was synthesized from **69**

(1.89 g, 8.10 mmol) according to general procedure B. **73** was obtained as a yellow oil: 1.50 g

(90%). ^{1}H-NMR (CDCl$_3$, 400 MHz) δ 1.34-1.37 (m, 2H), 1.49-1.52 (m, 4H), 2.27-2.31 (m, 4H), 3.38 (s, 2H), 4.55 (s, 2H), 7.18-7.22 (m, 4H).

(4-((4-Methylpiperazin-1-yl)methyl)phenyl)methanol (74). The title compound was synthesized from **70** (2.10 g, 8.45 mmol) according to general procedure B. Elution with DCM/MeOH/33% aqueous NH$_3$ solution (9:1:0.2) afforded **74** as a white solid: 1.44 g (77%). ^{1}H-NMR (CDCl$_3$, 400 MHz) δ 2.11 (s, 3H), 2.28-2.32 (m, 8H), 3.38 (s, 2H), 4.52 (s, 2H), 7.18-7.23 (m, 4H).

General procedure (C) for the synthesis of benzaldehydes 52-55.

To a -78 °C solution of oxalyl chloride (1.2 eq.) in DCM (0.5 M) anhydrous DMSO (4.0 eq.) in DCM (0.5 M) was slowly added. After stirring for 15 min, the reaction mixture was added to a solution of the proper alcohol (**71-74**) (1.0 eq.) in DCM (0.4 M) and allowed to stir at -78 °C for 1 h. Et$_3$N (5.0 eq.) was subsequently added and the resulting mixture was stirred at -78 °C for additional 20 min and then warmed up to rt. The reaction medium was diluted with H$_2$O (30 mL), and the immiscible phases were separated over a separatory funnel. The organic layer was washed with brine (30 mL), dried over anhydrous Na$_2$SO$_4$, filtered and concentrated under vacuum to afford the title compound (**52-55**). Further purification by flash chromatography was performed when required.

4-((Diethylamino)methyl)benzaldehyde (52). The title compound was synthesized from **71** (0.83 g, 4.20 mmol) according to general procedure C. **52** was obtained as a yellow oil: 0.48 g

(60%). ^{1}H-NMR (CDCl$_3$, 200 MHz) δ 0.91 (t, J = 7.0 Hz, 6H), 2.43 (q, J = 6.6 Hz, 4H), 3.54 (s, 2H), 7.41 (d, J = 7.8 Hz, 2H), 7.65 (d, J = 7.8, 2H), 9.80 (s, 1H).

4-(Morpholinomethyl)benzaldehyde (53). The title compound was synthesized from **72** (1.40 g, 6.75 mmol) according to general procedure C. Elution with DCM/MeOH/33% aqueous NH$_3$ solution (9.5:0.5:0.03) afforded **5** as a yellow solid: 0.81 g (59%). ^{1}H-NMR (CDCl$_3$, 400 MHz) δ 2.36-2.38 (m, 4H), 3.49 (s, 2H), 3.61-3.64 (m, 4H), 7.43 (d, J = 8.0 Hz, 2H), 7.75 (d, J = 8.0 Hz, 2H), 9.90 (s, 1H). ^{13}C-NMR (CDCl$_3$, 100 MHz) δ 53.6, 62.9, 66.8, 129.4, 129.7, 135.5, 145.3, 191.8.

4-(Piperidin-1-ylmethyl)benzaldehyde (54). The title compound was synthesized from **73** (1.18 g, 5.74 mmol) according to general procedure C. Elution with DCM/MeOH/33% aqueous NH$_3$ solution (9.5:0.5:0.03) afforded **54** as a yellow oil: 0.92 g (79%). ^{1}H-NMR (CDCl$_3$, 400 MHz) δ 1.28-1.32 (m, 2H), 1.44-1.48 (m, 4H), 2.23-2.27 (m, 4H), 3.40 (s, 2H), 7.38 (d, J = 7.2 Hz, 2H), 7.69 (d, J = 7.2 Hz, 2H), 9.86 (s, 1H).

4-((4-Methylpiperazin-1-yl)methyl)benzaldehyde (55). The title compound was synthesized from **74** (1.44 g, 6.53 mmol) according to general procedure C. Elution with DCM/MeOH/33% aqueous NH$_3$ solution (9:1:0.1) afforded **55** as a yellow oil: 1.25 g (88%). ^{1}H-NMR (CDCl$_3$, 400 MHz) δ 2.20 (s, 3H), 2.26-2.56 (m, 8H), 3.49 (s, 2H), 7.42 (d, J = 7.6 Hz, 2H), 7.74 (d, J = 7.6 Hz, 2H), 9.90 (s, 1H). ^{13}C-NMR (CDCl$_3$, 100 MHz) δ 45.9, 53.1, 55.0, 62.5, 129.3, 129.6, 135.4, 145.7, 191.8.

General procedure (F) for the synthesis of *N*-cyano-*N'*-alkyl/arylguanidines (78-80). To a suspension of sodium dicyanamide (**81**) (1.2 eq.) in 1-butanol (1.2 M), the proper amine hydrochloride (**82-84**) (1.0 eq.) was added. The resulting mixture was heated at reflux for 6-8 h, affording a white precipitate, which was filtered off. The filtrate was concentrated under vacuum to yield crude *N*-cyano-*N'*-alkyl/arylguanidine (**78-80**). Further purification methods were employed when required.

N-Cyano-*N'*-ethylguanidine (78). The title compound was obtained according to general procedure F using ethylamine hydrochloride **82** (2.29 g, 27.07 mmol). Elution with DCM/MeOH/33% aqueous NH_3 solution (9:1:0.1) afforded **78** as a yellow oil: 2.5 g (73%). ^{1}H-NMR (D_2O, 400 MHz) δ 1.19 (t, $J = 6.8$ Hz, 3H), 3.23 (q, $J = 6.8$ Hz, 2H). ^{13}C-NMR (D_2O, 100 MHz) δ 13.3, 36.5, 120.5, 161.1.

N-Cyano-*N'*-propylguanidine (79). The title compound was obtained according to general procedure F using propylamine hydrochloride **83** (2.30 g, 24.53 mmol). Elution with DCM/MeOH/33% aqueous NH_3 solution (9:1:0.1) afforded **79** as a waxy solid: 1.9 g (63%). ^{1}H-NMR (CD_3OD, 400 MHz) δ 0.90 (t, $J = 7.2$ Hz, 3H), 1.49-1.54 (m, 2H), 3.09 (t, $J = 6.8$ Hz, 2H). ^{13}C-NMR (CD_3OD, 100 MHz) δ 10.1, 22.2, 42.8, 118.8, 161.7.

N-Cyano-*N'*-phenylguanidine (80). The title compound was obtained according to general procedure F using aniline hydrochloride **84** (0.65 g, 5.05 mmol). The crude material was triturated with H_2O, affording **80** as a white solid, which was used in the next step without further purification: 0.80 g (quantitative yield). ^{1}H-NMR (DMSO-d_6, 400 MHz) δ 6.98 (br s,

exch, 2H), 7.05-7.09 (m, 1H), 7.28-7.35 (m, 2H), 9.03 (br s, exch, 1H). ^{13}C-NMR (DMSO-d_6, 100 MHz) δ 117.6, 121.7, 124.2, 129.2, 138.4, 159.9.

***N*-Guanylurea sulfate hydrate (36).** To a solution of cyanoguanidine (**35**) (1.0 g, 11.9 mmol) in water (8 mL) 70% aqueous H$_2$SO$_4$ (3.30 g, 23.8 mmol.) was added. The resulting mixture was stirred at rt for 15 min and heated at reflux for 45 min. The reaction mixture was then cooled to rt, affording the precipitation of a white solid, which was collected by filtration. The residue was triturated with Et$_2$O, and used in the next step without further purification. **36** was obtained as a white solid: 2.20 g (93%). Mp: 199 (dec.) ^{1}H NMR (400 MHz; DMSO-d_6): δ 6.92 (br s, exch, 2H), 8.23 (br s, exch, 4H), 11.38 (br s, exch, 1H); ^{13}C NMR (100 MHz; DMSO-d_6): δ 155.4, 156.1; MS (ESI) m/z 103 [M + H]$^+$.

General procedure (G) for the synthesis of *N'*-alkyl/arylguanylureas (85-87). To a solution of cyanoguanidine (**78-80**) (1.0 eq.) in water (1.2 M) 70% aqueous sulfuric acid (2.0 eq.) was added. The resulting mixture was stirred at rt for 15 min and heated at reflux for 1 h. The reaction mixture was then cooled to rt and basified with Na$_2$CO$_3$. The aqueous phase was evaporated *in vacuo*, and the crude material was taken up with MeOH. The residue was filtered off and the organic solvent was concentrated under vacuum, to afford the title compound (**85-87**), which was used in the next step without further purification.

(*N'*-Ethylcarbamimidoyl)urea (85). The title compound was obtained according to general procedure G using **78** (2.50 g, 20.46 mmol). **85** was obtained as a gummy solid: 3.90 g

(quantitative yield). ^{1}H-NMR (D$_2$O, 400 MHz) δ 0.48 (t, J = 6.8 Hz, 3H), 2.58 (q, J = 6.8 Hz, 2H). ^{13}C-NMR (D$_2$O, 100 MHz) δ 12.1, 35.8, 152.8, 155.2.

(*N*'-Propylcarbamimidoyl)urea (86). The title compound was obtained according to general procedure G using **79** (1.80 g, 14.26 mmol). **86** was obtained as a gummy solid: 2.40 g (quantitative yield). ^{1}H-NMR (D$_2$O, 400 MHz) δ 0.49-0.54 (m, 3H), 1.14-1.25 (m, 2H), 2.71 (t, J = 6.8 Hz, 1H), 2.83 (t, J = 6.8 Hz, 1H). ^{13}C-NMR (D$_2$O, 100 MHz) δ 10.1, 21.1, 42.6, 155.7, 156.3.

(*N*'-Phenylcarbamimidoyl)urea (87). The title compound was obtained according to general procedure G using **80** (0.80 g, 4.90 mmol). **87** was obtained as a white solid: 0.72 g (82%).^{1}H-NMR (CDCl$_3$, 400 MHz) δ 7.01-7.06 (m, 3H), 7.21-7.25 (m, 2H). ^{13}C-NMR (CDCl$_3$, 100 MHz) δ 124.0, 125.0, 129.5, 140.0, 155.6, 163.6.

General procedure (H) for the synthesis of 6-amino-4-aryl-3,4-dihydro-1,3,5-triazin-2(1*H*)-ones (3-27), 6-amino-4aryl-3,4-dihydro-1,3,5-triazine-2(1*H*)-thiones (28-31) and 6-*N*-alkyl/aryl-4-aryl-3,4-dihydro-1,3,5-triazin-2(1*H*)-ones (32-34). To a solution of *N*-guanylurea sulfate hydrate (**36**), or 2-imino-4-thiobiuret (**75**), or *N*'-alkyl/arylguanylurea (**85-87**) (1.0 eq.) in concentrated H$_2$SO$_4$ (5.5 M) the proper benzaldehyde (**37-61**, **76**, and **77**) (1.2 eq.) was added. After stirring at rt for 72 h, the reaction mixture was diluted with a small amount of cold H$_2$O. The solution was then made basic with Na$_2$CO$_3$, affording a precipitate which was collected by filtration. Whereas no precipitation was observed, the aqueous phase was concentrated *in vacuo*.

The crude material was either purified by trituration with organic solvents or by chromatographic techniques affording the title compound (**3-34**).

6-Amino-4-(2-nitrophenyl)-3,4-dihydro-1,3,5-triazin-2(1*H*)-one (3). The title compound was obtained according to general procedure H using 2-nitrobenzaldehyde (**37**) (0.91 g, 6.00 mmol) and **36** (0.80 g, 5.00 mmol). The crude material was triturated with a mixture of Et_2O/DCM and washed with H_2O to afford **3** as a brown solid: 0.19 g (16%). ^{1}H NMR (400 MHz; DMSO-d_6): δ 5.62 (br s, exch, 2H), 6.16 (s, 1H), 7.54-7.59 (m, 3H), 7.74 (t, *J* = 8.0 Hz, 1H), 7.91 (d, *J* =8.0 Hz, 1H), 8.78 (br s, exch, 1H). ^{13}C NMR (100 MHz; DMSO-d_6): δ 64.1, 124.0, 126.9, 128.3, 132.6, 137.5, 147.4, 149.9, 153.3. MS (ESI) *m/z* 236 [M + H][+].

6-Amino-4-(3-nitrophenyl)-3,4-dihydro-1,3,5-triazin-2(1*H*)-one (4). The title compound was obtained according to general procedure H using 3-nitrobenzaldehyde (**38**) (0.91 g, 6.00 mmol) and **36** (0.80 g, 5.00 mmol). The crude material was triturated with a mixture of Et_2O/DCM and washed with H_2O to afford **4** as a white solid: 0.63 g (53%). ^{1}H NMR (400 MHz; DMSO-d_6): δ 5.47 (br s, exch, 2H), 5.73 (br s, 1H), 7.66 (t, *J* = 8.0 Hz, 1H), 7.73 (br s, exch, 1H), 7.80 (d, *J* = 8.0 Hz, 1H), 8.15 (d, *J* = 8.0 Hz, 1H), 8.19 (s, 1H), 8.86 (br s, exch, 1H). ^{13}C NMR (100 MHz; DMSO-d_6): δ 67.1, 120.6, 122.2, 129.7, 132.9, 147.8, 148.1, 150.2, 153.6. MS (ESI) *m/z* 236 [M + H][+], MS (ESI) *m/z* 234 [M - H][-].

6-Amino-4-(4-nitrophenyl)-3,4-dihydro-1,3,5-triazin-2(1*H*)-one (5). The title compound was obtained according to general procedure H using 4-nitrobenzaldehyde (**39**) (0.23 g, 1.50 mmol) and **36** (0.20 g, 1.25 mmol). The crude material was triturated with a mixture of Et_2O/DCM and

washed with H_2O to afford **5** as a white solid: 53 mg (22%). ^{1}H NMR (400 MHz; DMSO-d_6): δ 5.92 (s, 1H), 7.65 (d, *J*= 8.0 Hz, 2H), 8.28 (d, *J* =8.0 Hz, 2H), 8.54 (br s, exch, 1H). ^{13}C NMR (100 MHz; DMSO-d_6): δ 64.0, 123.8, 127.6, 147.5, 148.9, 150.7, 152.3. MS (ESI) *m/z* 236 [M + H][+], MS (ESI) *m/z* 234 [M - H][-].

6-Amino-4-(2-bromophenyl)-3,4-dihydro-1,3,5-triazin-2(1*H*)-one (6). The title compound was obtained according to general procedure H using 2-bromobenzaldehyde (**40**) (0.70 mL, 6.00 mmol) and **36** (0.80 g, 5.00 mmol). The crude material was triturated with a mixture of Et_2O/DCM and washed with H_2O to afford **6** as a white solid: 0.73 g (54%). ^{1}H NMR (400 MHz; DMSO-d_6): δ 5.68 (br s, exch, 2H), 5.88 (s, 1H), 7.22-7.26 (m, 1H), 7.41 (d, *J* = 8.0 Hz, 2H), 7.46 (br s, exch, 1H), 7.58 (d, *J* = 8.0 Hz, 1H), 8.62 (br s, exch, 1H). ^{13}C NMR (100 MHz; DMSO-d_6): δ 67.6, 120.6, 127.6, 129.3, 132.4, 134.6, 141.6, 149.4, 153.0.

6-Amino-4-(3-bromophenyl)-3,4-dihydro-1,3,5-triazin-2(1*H*)-one (7). The title compound was obtained according to general procedure H using 3-bromobenzaldehyde (**41**) (0.56 mL, 4.80 mmol) and **36** (0.60 g, 4.00 mmol). The crude material was triturated with a mixture of Et_2O/DCM and washed with H_2O to afford **7** as a white solid: 0.40 g (38%). ^{1}H NMR (400 MHz; DMSO-d_6): δ 5.64 (s, 1H), 7.34-7.36 (m, 2H), 7.50-7.53 (m, 2H), 7.88 (br s, exch, 1H). ^{13}C NMR (100 MHz; DMSO-d_6): δ 66.6, 121.8, 125.7, 129.2, 131.2, 131.3, 145.9, 152.0, 153.6.

6-Amino-4-(2-fluorophenyl)-3,4-dihydro-1,3,5-triazin-2(1*H*)-one (8). The title compound was obtained according to general procedure H using 2-fluorobenzaldehyde (**42**) (0.50 mL, 4.80 mmol) and **36** (0.64 g, 4.00 mmol). The crude material was triturated with a mixture of

1
2
3
4
5
6
7
8
9
10
11
12
13
14
15
16
17
18
19
20
21
22
23
24
25
26
27
28
29
30
31
32
33
34
35
36
37
38
39
40
41
42
43
44
45
46
47
48
49
50
51
52
53
54
55
56
57
58
59
60

Et_2O/DCM and washed with H_2O to afford **8** as a white solid: 0.52 g (62%). ^1H NMR (400 MHz; DMSO-d_6): δ 5.39 (br s, exch, 2H), 5.83 (s, 1H), 7.12-7.21 (m, 2H), 7.30-7.37 (m, 2H), 7.48 (br s, exch, 1H), 8.80 (br s, exch, 1H). ^{13}C NMR (100 MHz; DMSO-d_6): δ 64.1, 125.1(d, J = 6.0 Hz), 125.7 (d, J = 29.0 Hz), 128.4, 129.0, 132.9, 150.1, 152.6, 159.1 (d, J = 234.0 Hz). MS (ESI) m/z 209 $[M + H]^+$.

6-Amino-4-(3-fluorophenyl)-3,4-dihydro-1,3,5-triazin-2(1*H*)-one (9). The title compound was obtained according to general procedure H using 3-fluorobenzaldehyde (**43**) (0.64 mL, 6.00 mmol) and **36** (0.80 g, 5.00 mmol). The crude material was triturated with a mixture of Et_2O/DCM and washed with H_2O to afford **9** as a white solid: 0.74 g (71%). ^1H NMR (400 MHz; DMSO-d_6): δ 5.47 (br s, exch, 2H), 5.57 (s, 1H), 7.08-7.12 (m, 2H), 7.17-7.19 (m, 1H), 7.36-7.42 (m, 1H), 7.56 (br s, exch, 1H), 8,85 (br s, exch, 1H). ^{13}C NMR (100 MHz; DMSO-d_6): δ 67.7, 112.6, 113.2, 121.6, 129.8, 147.9, 150.4, 152.3, 161.0 (d, J = 246.0 Hz). MS (ESI) m/z 209 $[M + H]^+$.

6-Amino-4-(2-(trifluoromethyl)phenyl)-3,4-dihydro-1,3,5-triazin-2(1*H*)-one (10). The title compound was obtained according to general procedure H using 2-trifluoromethylbenzaldehyde (**44**) (0.63 mL, 4.80 mmol) and **36** (0.64 g, 4.00 mmol). The crude material was triturated with a mixture of Et_2O/DCM and washed with H_2O to afford **10** as a white solid: 0.13 g (12%). ^1H NMR (400 MHz; DMSO-$d6$): δ 5.93 (br s, 3H), 7.51-7.54 (m, 1H), 7.66 (br s, 1H), 7.70-7.76 (m, 3H). ^{13}C NMR (100 MHz; DMSO-$d6$): δ 64.1, 124.3, 125.1, 125.6, 128.4, 129.0, 132.9, 142.1, 150.1, 152.6. MS (ESI) m/z 259 $[M + H]^+$; MS (ESI) m/z 257 $[M - H]^-$.

6-Amino-4-(3-(trifluoromethyl)phenyl)-3,4-dihydro-1,3,5-triazin-2(1*H*)-one (11). The title compound was obtained according to general procedure H using 3-trifluoromethylbenzaldehyde (**45**) (0.80 mL, 6.00 mmol) and **36** (0.80 g, 5.00 mmol). The crude material was triturated with a mixture of Et$_2$O/DCM and washed with H$_2$O to afford **11** as a white solid: 0.68 g (50%). ^{1}H NMR (400 MHz; DMSO-*d*6): δ 5.68 (s, 1H), 5.81 (br s, exch, 2H), 7.58-7.68 (m, 5H), 8.63 (br s, exch, 1H). ^{13}C NMR (100 MHz; DMSO-*d*6): δ 67.0, 122.3, 123.2, 124.1, 126.2, 128.9, 130.4, 144.8, 150.5, 153.5. MS (ESI) *m/z* 259 [M + H]$^+$; MS (ESI) *m/z* 257 [M - H]$^-$.

6-Amino-4-(2-chlorophenyl)-3,4-dihydro-1,3,5-triazin-2(1*H*)-one (12). The title compound was obtained according to general procedure H using 2-chlorobenzaldehyde (**46**) (0.54 mL, 4.80 mmol) and **36** (0.64 g, 4.00 mmol). The crude material was triturated with a mixture of Et$_2$O/DCM and washed with H$_2$O to afford **12** as a white solid: 0.58 g (64%). ^{1}H NMR (400 MHz; DMSO-*d*$_6$): δ 5.56 (br s, exch, 2H), 5.91 (s, 1H), 7.30-7.42 (m, 5H), 8.87 (br s, exch, 1H). ^{13}C NMR (100 MHz; DMSO-*d*$_6$): δ 65.6, 127.1, 127.6, 128.8, 128.9, 131.8, 141.3, 149.1, 153.1. MS (ESI) *m/z* 225 [M + H]$^+$; MS (ESI) *m/z* 223 [M - H]$^-$.

6-Amino-4-(3-chlorophenyl)-3,4-dihydro-1,3,5-triazin-2(1*H*)-one (13). The title compound was obtained according to general procedure H using 3-chlorobenzaldehyde (**47**) (0.43 mL, 3.75 mmol) and **36** (0.50 g, 3.12 mmol). The crude material was triturated with a mixture of Et$_2$O/DCM and washed with H$_2$O to afford **13** as a white solid: 0.43 g (61%). ^{1}H NMR (400 MHz; DMSO-*d*$_6$): δ 5.57 (s, 1H), 5.76 (br s, exch, 2H), 7.29-7.41 (m, 4H), 7.59 (br s, exch, 1H), 8.60 (br s, exch, 1H). ^{13}C NMR (100 MHz; DMSO-*d*$_6$): δ 67.7, 125.2, 125.9, 127.6, 130.5, 133.1, 147.0, 151.3, 154.3. MS (ESI) *m/z* 225 [M + H]$^+$.

1
2
3
4
5
6
7
8
9
10
11
12
13
14
15
16
17
18
19
20
21
22
23
24
25
26
27
28
29
30
31
32
33
34
35
36
37
38
39
40
41
42
43
44
45
46
47
48
49
50
51
52
53
54
55
56
57
58
59
60

6-Amino-4-(4-chlorophenyl)-3,4-dihydro-1,3,5-triazin-2(1*H*)-one (14). The title compound was obtained according to general procedure H using 4-chlorobenzaldehyde (**48**) (0.67 g, 4.80 mmol) and **36** (0.64 g, 4.00 mmol). The crude material was triturated with a mixture of Et_2O/DCM and washed with H_2O to afford **14** as a white solid: 0.61 g (67%). ^{1}H NMR (400 MHz; DMSO-d_6): δ 5.55 (s, 1H), 5.56 (br s, exch, 2H), 7.34 (d, J = 8.0 Hz, 2H), 7.41 (d, J = 8.0 Hz, 2H), 7.53 (br s, exch, 1H), 8.93 (br s, exch, 1H) . ^{13}C NMR (100 MHz; DMSO-d_6): δ 67.4, 127.7, 127.8, 131.6, 143.2, 148.8, 153.3. MS (ESI) *m/z* 225 [M + H]$^{+}$.

6-Amino-4-(*o*-tolyl)-3,4-dihydro-1,3,5-triazin-2(1*H*)-one (15). The title compound was obtained according to general procedure H using *o*-tolylbenzaldehyde (**49**) (0.70 mL, 6.00 mmol) and **36** (0.80 g, 5.00 mmol). The crude material was triturated with a mixture of Et_2O/DCM and washed with H_2O to afford **15** as a white solid: 0.34 g (33%). ^{1}H NMR (400 MHz; DMSO-d_6): δ 2.37 (s, 3H), 5.88 (s, 1H), 7.17-7.20 (m, 1H), 7.21-7.26 (m, 2H), 7.29-7.32 (m, 1H), 7.84 (br s, exch, 1H). ^{13}C NMR (100 MHz; DMSO-d_6): δ 19.2, 62.4, 126.1, 126.2, 128.2, 130.1, 35.4, 138.8, 152.0, 153.4. MS (ESI) *m/z* 205 [M + H]$^{+}$.

6-Amino-4-(*m*-tolyl)-3,4-dihydro-1,3,5-triazin-2(1*H*)-one (16). The title compound was obtained according to general procedure H using *m*-tolylbenzaldehyde (**50**) (0.71 mL, 6.00 mmol) and **36** (0.80 g, 5.00 mmol). The crude material was triturated with a mixture of Et_2O/DCM and washed with H_2O to afford **16** as a white solid: 0.34 g (33%). ^{1}H NMR (400 MHz; DMSO-d_6): δ 2.31 (s, 3H), 5.62 (s, 1H), 7.14-7.18 (m, 3H), 7.25-7.28 (m, 1H), 7.97 (br s,

exch, 1H). ^{13}C NMR (100 MHz; DMSO-d_6): δ 21.2, 66.5, 122.8, 126.8, 128.0, 128.4, 137.9, 141.9, 152.9, 153.9. MS (ESI) *m/z* 205 [M + H]$^+$.

6-Amino-4-(3-(dimethylamino)phenyl)-3,4-dihydro-1,3,5-triazin-2(1*H*)-one (17). The title compound was obtained according to general procedure H using 3-(dimethylamino)benzaldehyde (**51**) (0.49 g, 3.33 mmol) and **36** (0.43 g, 2.70 mmol). The crude material was triturated with a mixture of Et$_2$O/DCM and washed with H$_2$O to afford **17** as a white solid: 0.30 g (48%). ^{1}H NMR (400 MHz; DMSO-d_6): δ 2.88 (s, 6H), 5.47 (s, 1H), 6.63-6.65 (m, 2H), 6.71 (s, 1H), 7.14 (t, *J* = 8.0 Hz, 1H), 7.35 (br s, exch, 1H). ^{13}C NMR (100 MHz; DMSO-d_6): δ 40.1, 66.3, 110.1, 111.3, 113.1, 128.2, 145.1, 150.8, 152.6, 154.2. MS (ESI) *m/z* 234 [M + H]$^+$.

6-Amino-4-(4-((diethylamino)methyl)phenyl)-3,4-dihydro-1,3,5-triazin-2(1*H*)-one (18). The title compound was obtained according to general procedure H using 4-((diethylamino)methyl)benzaldehyde (**52**) (0.48 g, 2.50 mmol) and **36** (0.33 g, 2.08 mmol). The crude material was purified by flash chromatography, eluting with DCM/MeOH/33% aqueous NH$_3$ solution (8:2:0.2) to afford **18** as a white solid: 0.32 g (57%). ^{1}H NMR (400 MHz; DMSO-d_6): δ 1.15 (t, *J* = 7.6 Hz, 6H), 2.82 (q, *J* = 7.6 Hz, 4H), 4.04 (s, 2H), 5.88 (s, 1H), 7.43 (d, *J* = 8.4 Hz, 2H), 7.62 (d, *J* = 8.4 Hz, 2H), 8.78 (br s, exch, 1H). ^{13}C NMR (100 MHz; DMSO-d_6): δ 11.6, 45.8, 56.3, 67.1, 125.3, 127.8, 139.7, 142.9, 155.0, 156.2. MS (ESI) *m/z* 276 [M + H]$^+$.

6-Amino-4-(4-(morpholinomethyl)phenyl)-3,4-dihydro-1,3,5-triazin-2(1*H*)-one (19). The title compound was obtained according to general procedure H using 4-

(morpholinomethyl)benzaldehyde (**53**) (0.81 g, 3.94 mmol) and **36** (0.52 g, 3.28 mmol). The crude material was triturated with a mixture of Et_2O/DCM and washed with H_2O to afford **19** as a white solid: 0.58 g (61%). ^{1}H NMR (400 MHz; DMSO-d_6): δ 2.32-2.34 (m, 4H), 3.43 (s, 2H), 3.54-3.57 (m, 4H), 5.53 (s, 1H), 7.26-7.28 (m, 4H), 7.42 (br s, exch, 1H). ^{13}C NMR (100 MHz; DMSO-d_6): δ 53.6, 62.7, 66.7, 68.0, 126.3, 128.9, 137.6, 143.3, 152.3, 154.2. MS (ESI) m/z 290 $[M + H]^+$.

6-Amino-4-(4-(piperidin-1-ylmethyl)phenyl)-3,4-dihydro-1,3,5-triazin-2(1H)-one (20). The title compound was obtained according to general procedure H using 4-(piperidin-1-ylmethyl)benzaldehyde (**54**) (0.92 g, 4.50 mmol) and **36** (0.60 g, 3.77 mmol). The crude material was triturated with a mixture of Et_2O/DCM and washed with H_2O to afford **20** as a white solid: 0.52 g (63%). ^{1}H NMR (400 MHz; DMSO-d_6): δ 1.35-1.40 (m, 2H), 1.45-1.50 (m, 4H), 2.27-2.30 (m, 4H), 2.38 (s, 2H), 5.33 (br s, exch, 2H), 5.52 (s, 1H), 7.24-7.26 (m, 4H), 7.53 (br s, exch, 1H), 8.87 (br, s, exch, 1H). ^{13}C NMR (100 MHz; DMSO-d_6): δ 24.0, 25.5, 54.2, 61.9, 68.6, 126.1, 128.4, 138.2, 143.7, 148.7, 153.1. MS (ESI) m/z 288 $[M + H]^+$.

6-Amino-4-(4-((4-methylpiperazin-1-yl)methyl)phenyl)-3,4-dihydro-1,3,5-triazin-2(1H)-one (21). The title compound was obtained according to general procedure H using 4-((4-methylpiperazin-1-yl)methyl)benzaldehyde (**55**) (1.25 g, 5.73 mmol) and **36** (0.76 g, 4.77 mmol). The crude material was triturated with a mixture of Et_2O/DCM and washed with H_2O to afford **21** as a white solid: 0.78 g (54%). ^{1}H NMR (400 MHz; DMSO-d_6): δ 2.14 (s, 3H), 2.28-2.32 (m, 8H), 3.42 (s, 2H), 5.41 (br s, exch, 2H), 5.53 (s, 1H), 7.24-7.26 (m, 4H), 7.44 (br s, exch, 1H),

8.80 (br s, exch, 1H). ^{13}C NMR (100 MHz; DMSO-d_6): δ 45.5, 52.3, 54.5, 61.6, 68.4, 125.5, 128.3, 138.0, 143.6, 148.8, 153.0. MS (ESI) m/z 303 [M + H]$^+$.

4-([1,1'-Biphenyl]-4-yl)-6-amino-3,4-dihydro-1,3,5-triazin-2(1H)-one (22). The title compound was obtained according to general procedure H using [1,1'-biphenyl]-4-carbaldehyde (**56**) (0.48 g, 2.55 mmol) and **36** (0.40 g, 2.13 mmol). The crude material was triturated with a mixture of Et$_2$O/DCM and washed with H$_2$O to afford **22** as a white solid: 0.15 g (26%). ^{1}H NMR (400 MHz; DMSO-d_6): δ 5.64 (s, 1H), 7.42-7.48 (m, 4H), 7.64-7.67 (m, 5H). ^{13}C NMR (100 MHz; DMSO-d_6): δ 66.9, 126.2, 126.6, 127.4, 128.6, 139.7, 140.8, 142.8, 150.7, 153.5. MS (ESI) m/z 267 [M + H]$^+$; MS (ESI) m/z 265 [M - H]$^-$.

6-Amino-4-(3,4-dichlorophenyl)-3,4-dihydro-1,3,5-triazin-2(1H)-one (23). The title compound was obtained according to general procedure H using 3,4-dichlorobenzaldehyde (**57**) (0.33 g, 1.87 mmol) and **36** (0.25 g, 1.56 mmol). The crude material was triturated with a mixture of Et$_2$O/DCM and washed with H$_2$O to afford **23** as a white solid: 0.32 g (80%). ^{1}H NMR (400 MHz; DMSO-d_6): δ 5.60 (s, 1H), 6.12 (br s, exch, 2H), 7.33 (d, J = 8.0 Hz, 2H), 7.55 (s, 1H), 7.63 (d, J = 8.0 Hz, 2H), 7.69 (br s, exch, 1H). ^{13}C NMR (100 MHz; DMSO-d_6): δ 66.3, 126.5, 127.5, 130.2, 131.4, 131.8, 144.8, 150.4, 152.9.

6-Amino-4-(3,5-difluorophenyl)-3,4-dihydro-1,3,5-triazin-2(1H)-one (24). The title compound was obtained according to general procedure H using 3,5-difluorobenzaldehyde (**58**) (0.31 g, 2.24 mmol) and **36** (0.30 g, 1.87 mmol). The crude material was triturated with a mixture of Et$_2$O/DCM and washed with H$_2$O to afford **24** as a white solid: 0.31 g (71%). ^{1}H

NMR (400 MHz; DMSO-d_6): δ 5.61 (s, 1H), 5.89 (br s, exch, 2H), 7.01-7.05 (m, 2H), 7.12-7.17 (m, 1H), 7.72 (br s, exch, 1H).^{13}C NMR (100 MHz; DMSO-d_6): δ 66.2, 102.5, 108.8, 147.3, 150.9, 154.2, 161.9 (d, J = 251.0). MS (ESI) *m/z* 227 [M + H]$^+$; MS (ESI) *m/z* 225 [M - H]$^-$.

6-Amino-4-(2,3-dihydrobenzo[*b*][1,4]dioxin-6-yl)-3,4-dihydro-1,3,5-triazin-2(1*H*)-one (25). The title compound was obtained according to general procedure H using 2,3-dihydrobenzo[*b*][1,4]dioxine-6-carbaldehyde (**59**) (0.78 g, 4.48 mmol) and **36** (0.64 g, 4.00 mmol). The crude material was triturated with a mixture of Et$_2$O/DCM and washed with H$_2$O to afford **25** as a white solid: 0.10 g (10%). ^{1}H NMR (400 MHz; DMSO-d_6): δ 4.21 (s, 4H), 5.42 (br s, 3H), 6.77-6.82 (m, 3H), 7.36 (br s, exch, 1H), 8.75 (br s, exch, 1H).^{13}C NMR (100 MHz; DMSO-d_6): δ 63.8, 68.0, 114.6, 116.6, 118.4, 142.9, 148.2, 151.9, 152.2.

6-Amino-4-(pyridin-3-yl)-3,4-dihydro-1,3,5-triazin-2(1*H*)-one (26). The title compound was obtained according to general procedure H using nicotinaldehyde (**60**) (0.56 mL, 6.00 mmol) and **36** (0.80 g, 5.00 mmol). The crude material was purified by flash chromatography, eluting with DCM/MeOH/33% aqueous NH$_3$ solution (5:4.5:0.5) to afford **26** as a white solid: 0.11 g (12%). ^{1}H NMR (400 MHz; CD$_3$OD): δ 6.45 (s, 1H), 7.37-7.40 (m, 1H), 7.86 (d, *J* = 8.0 Hz, 1H), 8.39-8.41 (m, 1H), 8.58 (s, 1H).^{13}C NMR (100 MHz; DMSO-d_6): δ 56.1, 122.4, 133.2, 139.3, 146.9, 147.0, 150.2, 152.5.

6-Amino-4-(pyridin-4-yl)-3,4-dihydro-1,3,5-triazin-2(1*H*)-one (27). The title compound was obtained according to general procedure H using isonicotinaldehyde (**61**) (0.57 mL, 6.00 mmol) and **36** (0.80 g, 5.00 mmol). The crude material was purified by flash chromatography, eluting

with DCM/MeOH/33% aqueous NH_3 solution (5:4.5:0.5) to afford **27** as a white solid: 0.12 g

(12%). ^{1}H NMR (400 MHz; CD_3OD): δ 6.41 (s, 1H), 7.46 (d, *J* =6.4 Hz, 2H), 8.46 (d, *J* = 6.4

Hz, 2H).^{13}C NMR (100 MHz; CD_3OD): δ 58.5, 121.6, 148.5, 152.4, 152.4, 152.8. MS (ESI) *m/z*

192 $[M + H]^+$.

6-Amino-4-phenyl-3,4-dihydro-1,3,5-triazine-2(1*H*)-thione (28). The title compound was

obtained according to general procedure H using benzaldehyde (**76**) (0.31 mL, 3.00 mmol) and

75 (0.30 g, 2.50 mmol). The crude material was purified by preparative HPLC/MS on prep C_{18}

column, using 10 mM NH_4OAc in H_2O at pH 5 adjusted with AcOH (A) and 10 mM NH_4OAc in

MeCN/H_2O (95:5) at pH 5 (B) as mobile phase. A linear gradient was applied starting at 0% B

(initial hold for 0.5 min) to 40% B in 7 min. From 40% to 100% B in 0.1 min and hold at 100%

for 2.4 min. The organic fractions were collected and concentrated under vacuum. The residue

was taken up with EtOAc, and washed with a saturated aqueous $NaHCO_3$ solution. The organic

phase was evaporated *in vacuo* to afford **28** as a white solid: 36 mg (7%). ^{1}H NMR (400 MHz;

DMSO-d_6): δ 5.55 (br s, 3H), 7.31-7.39 (m, 6H), 9.64 (br s, exch, 1H).^{13}C NMR (100 MHz;

DMSO-d_6): δ 68.8, 125.7, 127.6, 127.8, 143.7, 145.8, 176.3. MS (ESI) *m/z* 207 $[M + H]^+$.

6-Amino-4-(2-fluorophenyl)-3,4-dihydro-1,3,5-triazine-2(1*H*)-thione (29). The title

compound was obtained according to general procedure H using 2-fluorobenzaldehyde (**42**)

(0.32 mL, 3.00 mmol) and **75** (0.30 g, 2.50 mmol). The crude material was purified by

preparative HPLC/MS on prep C_{18} column, using 10 mM NH_4OAc in H_2O at pH 5 adjusted with

AcOH (A) and 10 mM NH_4OAc in MeCN/H_2O (95:5) at pH 5 (B) as mobile phase. A linear

gradient was applied starting at 0% B (initial hold for 0.5 min) to 40% B in 7 min. From 40% to

100% B in 0.1 min and hold at 100% for 2.4 min. The organic fractions were collected and concentrated under vacuum. The residue was taken up with EtOAc, and washed with a saturated aqueous $NaHCO_3$ solution. The organic phase was evaporated *in vacuo* to afford **29** as a white solid: 23 mg (3%). ^{1}H NMR (400 MHz; DMSO-d_6): δ 5.55 (br s, exch, 2H), 5.80 (s, 1H), 7.15-7.38 (m, 4H), 9.43 (br s, exch, 1H), 9.85 (br s, exch, 1H).^{13}C NMR (100 MHz; DMSO-d_6): δ 64.9, 115.9, 124.8, 128.2, 130.3, 145.3, 149.5, 159.2 (d, $J = 257$ Hz), 174.4. MS (ESI) *m/z* 225 [M + H]$^+$.

6-Amino-4-(4-fluorophenyl)-3,4-dihydro-1,3,5-triazine-2(1*H*)-thione (30). The title compound was obtained according to general procedure H using 4-fluorobenzaldehyde (**77**) (0.33 mL, 3.00 mmol) and **75** (0.30 g, 2.50 mmol). The crude material was purified by preparative HPLC/MS on prep C_{18} column, using 10 mM NH_4OAc in H_2O at pH 5 adjusted with AcOH (A) and 10 mM NH_4OAc in MeCN/H_2O (95:5) at pH 5 (B) as mobile phase. A linear gradient was applied starting at 0% B (initial hold for 0.5 min) to 40% B in 7 min. From 40% to 100% B in 0.1 min and hold at 100% for 2.4 min. The organic fractions were collected and concentrated under vacuum. The residue was taken up with EtOAc, and washed with a saturated aqueous $NaHCO_3$ solution. The organic phase was evaporated *in vacuo* to afford **30** as a white solid: 18 mg (3%). ^{1}H NMR (400 MHz; DMSO-d_6): δ 5.56 (s, 1H), 5.64 (br s, exch, 2H), 7.17-7.21 (m, 2H), 7.31-7.35 (m, 2H), 9.45 (br s, exch, 1H), 9.77 (br s, exch, 1H).^{13}C NMR (100 MHz; DMSO-d_6): δ 68.7, 115.0, 128.6, 140.4, 145.7, 162.3 (d, $J = 260$ Hz), 176.5. MS (ESI) *m/z* 225 [M + H]$^+$; MS (ESI) *m/z* 223 [M - H]$^-$.

6-Amino-4-(*o*-tolyl)-3,4-dihydro-1,3,5-triazine-2(1*H*)-thione (31). The title compound was obtained according to general procedure H using *o*-tolylbenzaldehyde (**49**) (0.46 mL, 4.06 mmol) and **75** (0.40 g, 3.38 mmol). The crude material was triturated with a mixture of Et$_2$O/DCM and washed with H$_2$O to afford **31** as a white solid: 0.49 g (66%). ^{1}H NMR (400 MHz; DMSO-d_6): δ 2.37 (s, 3H), 5.93 (s, 1H), 7.20-7.28 (m, 4H), 9.95 (br s, exch, 1H).^{13}C NMR (100 MHz; DMSO-d_6): δ 19.0, 64.4, 126.8, 128.8, 128.6, 131.5, 136.6, 138.3, 149.6, 175.5. MS (ESI) *m/z* 221 [M + H]$^+$.

6-(Ethylamino)-4-(*o*-tolyl)-3,4-dihydro-1,3,5-triazin-2(1*H*)-one (32). The title compound was obtained according to general procedure H using *o*-tolylbenzaldehyde (**49**) (0.36 mL, 3.19 mmol) and **85** (0.34 g, 2.65 mmol). Elution with DCM/MeOH/33% aqueous NH$_3$ solution (9:1:0.1) afforded **32** as a white solid: 0.26 g (43%). ^{1}H-NMR (DMSO-d_6, 400 MHz) δ 1.02 (t, *J* = 8.0 Hz, 3H), 2.37 (s, 3H), 3.05 (q, *J* = 8.0 Hz, 2H), 5.32 (br s, exch, 1H), 5.77 (s, 1H), 7.14-7.16 (m, 3H), 7.25-7.27 (m, 1H), 7.35 (br s, exch, 1H), 8.48 (br s, exch, 1H). ^{13}C-NMR (DMSO-d_6, 100 MHz) δ 15.4, 19.1, 35.3, 67.1, 126.4, 126.6, 130.7, 131.3, 135.7, 141.9, 148.3, 153.5. MS (ESI) *m/z* 233 [M + H]$^+$.

4-(4-Fluorophenyl)-6-(propylamino)-3,4-dihydro-1,3,5-triazin-2(1*H*)-one (33). The title compound was obtained according to general procedure H using 4-fluoro-benzaldehyde (**77**) (0.36 mL, 3.32 mmol) and **86** (0.40 g, 2.77 mmol). Elution with DCM/MeOH/33% aqueous NH$_3$ solution (9:1:0.1) afforded **33** as a white solid: 0.11 g (16%). ^{1}H-NMR (DMSO-d_6, 400 MHz) δ 0.84 (t, *J* = 7.2 Hz, 3H), 1.40-1.49 (m, 2H), 3.03 (t, *J* = 6.0 Hz, 2H), 5.59 (s, 1H), 5.75 (br s, exch, 1H), 7.14-7.18 (m, 2H), 7.34-7.38 (m, 2H), 7.55 (br s, exch, 1H), 8.55 (br s, exch, 1H).

^{13}C-NMR (DMSO-d_6, 100 MHz) δ 11.8, 22.7, 42.3, 68.1, 115.4 (d, J = 22.0 Hz), 128.6 (d, J = 8.0 Hz), 141.2, 149.0, 153.8, 161.6 (d, J = 244.0 Hz). MS (ESI) m/z 251 [M + H]$^{+}$.

4-(4-Fluorophenyl)-6-(phenylamino)-3,4-dihydro-1,3,5-triazin-2(1H)-one (34). The title compound was obtained according to general procedure H using 4-fluoro-benzaldehyde (**77**) (0.30 mL, 2.70 mmol) and **87** (0.40 g, 2.24 mmol). Elution with DCM/MeOH (9:1) afforded **34** as a white solid: 0.06 g (10%). ^{1}H-NMR (DMSO-d_6, 400 MHz) δ 5.78 (s, 1H), 6.89-6.92 (m, 1H), 7.17-7.24 (m, 4H), 7.41-7.45 (m, 2H), 7.52-7.54 (m, 2H), 7.82 (br s, exch, 1H), 8.02 (br s, exch, 1H), 8.52 (br s, exch, 1H). ^{13}C-NMR (DMSO-d_6, 100 MHz) δ 68.3, 114.6 (d, J = 21.0 Hz), 118.1, 121.3, 128.2 (d, J = 9.0 Hz), 128.6, 140.0, 145.11, 145.6, 152.1, 162.0 (d, J = 240.2 Hz). MS (ESI) m/z 285 [M + H]$^{+}$; MS (ESI) m/z 283 [M − H]$^{-}$.

X-ray analysis. Crystal data for **2**: formula $C_{11}H_{13}FN_4O.1/2$ H_2O, formula weight 244.25 uma, crystallographic system: monoclinic, space group C2/c, unit cell parameters: a = 26.784(2), b = 8.6624(5), c = 23.718(1) Å, β = 111.85(1)°, Z= 8, T= 293 K.

Crystals of **2,** suitable for the X-ray diffraction studies, were grown on slow evaporation of a water solution of the compound. Preliminary examination and data collection were carried out at rt on an Sapphire CCD detector (Oxford Diffraction Ltd., Agilent Technologies, USA) with MoKα radiation, λ = 0.71073 Å, monochromator graphite. Data reduction was automatically performed with CrysAlisPRO (Oxford Diffraction Ltd., UK). Cell parameters were obtained and refined by using PHICHI[57] and DIRAX[58] programs, respectively, catching reflections with random orientation in *hkl* planes. Intensities were corrected for Lorentz polarization and adsorption with the SADABS (G.M. Sheldrick *SADABS*, University of Gottingen, Germany,

2004) program. The XPREP (G.M. Sheldrick *XPREP* - Bruker-Nonius AXS , Madison, WI, USA, 2005) program was used for analysis of the data reduction and revealed a monoclinic C space group. The structure was solved by direct methods using the SHELXS97[59] program. SHELX- 97[59] was used for structure refinement based on F^2. The asymmetric unit contains two crystallographically independent molecules, A and B, and a water molecule. A and B are both different tautomers at the *endo-* or *exo-* double bond location in the triazinone ring and different conformers. While B shows clearly the double bond located at N(3)- C(9), A exhibits a 50:50 mixture of both tautomers. Large thermal vibrations characterize especially phenyl rings in both molecules. Attempting to solve disorder, a low temperature (100 K) data collection, and a second rt data collection with CuKα radiation were carried out. However, using the new data sets, no significant model improvement was achieved. Thus, we used the previous data set, although no satisfactory alternative model could be refined for A, despite repeated attempts. On the other hand, for the phenyl ring of B two different conformations were found, which could be independently refined.

The two independent molecules and the water molecule were then separately refined by blocked-matrix least-squares refinement until convergence, giving to each correspondent atom the same crystallographic numbering, with A and B labels, respectively. Non-hydrogen atoms were refined anisotropically. Hydrogen atoms bound to N- or C- atoms were positioned geometrically, giving 0.5 occupation factor to the different hydrogen positions in the *exo-/endo* mixed A molecule.

Final R indices for 327 parameters refined were R = 0.009 for all data and 0.0065 for 2217 observed (I > 4 sigma I) reflections, wR = 0.024 for all data and 0.018 for the observed ones, GooF S= 1.09. Molecular graphics were prepared using ORTEP-3 for Windows.[60]

1
2
3
4
5
6
7
8
9
10
11
12
13
14
15
16
17
18
19
20
21
22
23
24
25
26
27
28
29
30
31
32
33
34
35
36
37
38
39
40
41
42
43
44
45
46
47
48
49
50
51
52
53
54
55
56
57
58
59
60

Biology. Inhibition of BACE-1. β-secretase (BACE-1, Sigma-Aldrich) inhibition studies were performed by employing a peptide mimicking APP sequence as substrate (methoxycoumarin-Ser-Glu-Val-Asn-Leu-Asp-Ala-Glu-Phe-Lys-dinitrophenyl, M-2420, Bachem, Germany). The following procedure was employed: 5 μL of test compound (or DMSO, if preparing a control well) were pre-incubated with 175 μL of enzyme (in 20 mM sodium acetate containing 3-[(3-cholamidopropyl)dimethylammonio]-1-propanesulfonate (CHAPS) 0.1% w/v) for 1 h at rt. The substrate (3 μM, final concentration) was then added and left to react for 15 min at 37 °C. The fluorescence signal was read at λ_{em} = 405 nm (λ_{exc} = 320 nm) using a Fluoroskan Ascent. The DMSO concentration in the final mixture maintained below 5% (v/v) guaranteed no significant loss of enzyme activity. The fluorescence intensities with and without inhibitor were compared and the percent inhibition due to the presence of test compounds was calculated. The background signal was measured in control wells containing all the reagents, except BACE-1 and subtracted. The % inhibition due to the presence of increasing test compound concentration was calculated by the following expression: 100-(IF_i / IF_o × 100) where IF_i and IF_o are the fluorescence intensities obtained for BACE-1 in the presence and in the absence of inhibitor, respectively. Inhibition curves were obtained by plotting the % inhibition versus the logarithm of inhibitor concentration in the assay sample, when possible. The linear regression parameters were determined and the IC_{50} extrapolated (GraphPad Prism 4.0, GraphPad Software Inc.). To demonstrate inhibition of BACE-1 activity a peptido-mimetic inhibitor (β-secretase inhibitor IV, Calbiochem, IC_{50} = 20 nM) was serially diluted into the reactions' wells.

Inhibition of GSK-3β. Human recombinant GSK-3β was purchased from Millipore (Millipore Iberica S.A.U.) The prephosphorylated polypeptide substrate GSM was purchased from Millipore (Millipore Iberica SAU). Kinase-Glo Luminescent Kinase Assay was obtained from Promega (Promega Biotech Iberica, SL). ATP and all other reagents were from Sigma-Aldrich. Assay buffer contained 50 mM 4-(2-hydroxyethyl)-1-piperazineethanesulfonic acid (HEPES) (pH 7.5), 1 mM ethylenediaminetetraacetic acid (EDTA), 1 mM ethylene glycol tetraacetic acid (EGTA), and 15 mM magnesium acetate. The method developed by Baki was followed[36] to analyze the inhibition of GSK-3β. Kinase-Glo assays were performed in assay buffer using white 96-well plates. In a typical assay, 10 μL of test compound (dissolved in DMSO at 1 mM concentration and diluted in advance in assay buffer to the desired concentration) and 10 μL (20 ng) of enzyme were added to each well followed by 20 μL of assay buffer containing 25 μM substrate and 1 μM ATP. The final DMSO concentration in the reaction mixture did not exceed 1%. After 30 min incubation at 30 °C, the enzymatic reaction was stopped with 40 μL of Kinase-Glo reagent. Glow-type luminescence was recorded after 10 min using a Fluoroskan Ascent multimode reader.

The activity is proportional to the difference of the total and consumed ATP. The inhibitory activities were calculated on the basis of maximal kinase (average positive) and luciferase (average negative) activities measured in the absence of inhibitor and in the presence of reference compound inhibitor (SB415286 Merck Millipore, IC_{50} = 55 nM) at total inhibition concentration (5 μM), respectively.[61]

The linear regression parameters were determined and the IC_{50} extrapolated (GraphPad Prism 4.0, GraphPad Software Inc.).

H4-APP$_{sw}$ cell cultures. H4-APP$_{sw}$ cells, a neuroglioma cell line expressing the double Swedish mutation (K595N/M596L) of human APP (APP$_{sw}$), were cultured in Opti-MEM® reduced serum medium (Gibco) supplemented with 5% fetal bovine serum (FBS), 2 mM L-glutamine, 100 U/mL penicillin, 100 μg/mL streptomycin (EuroClone), 200 μg/mL hygromycin B (Sigma-Aldrich) and 2.5 μg/mL blasticidin S (Invitrogen), and maintained at 37 °C in a humidified atmosphere of 5% CO_2 and 95% air.

MTT assay. H4-APP$_{sw}$ cells were seeded onto 96-well plates (∼4.5 × 10^4 cells/well) and allowed to grow to 80% confluence. Cells were treated with **2** at 16 μM in 0.2% DMSO, **9** at 10 μM in 0.2% DMSO, **33** at 37 μM in 0.2% DMSO, β-secretase inhibitor IV at 25 μM in 0.2% DMSO, SB216763 at 10 μM in 0.2% DMSO or vehicles alone for 24 h. Cell survival was assayed by measuring the conversion of the yellow, water-soluble 3-(4,5-dimethylthiazol-2-yl)-2,5-diphenyltetrazolium bromide (MTT) (Sigma-Aldrich) to the blue, water-insoluble formazan. MTT assay was performed incubating cells with MTT solution for 4 h at 37 °C. Formazans were solubilized in DMSO. Data are presented as the percentage of survival relative to untreated control cultures. MTT assay was performed in triplicates.

ELISA assay. H4-APP$_{sw}$ cells were seeded onto 35 mm culture dishes (∼7 × 10^5 cells/dish) and allowed to grow to 80% confluence. Cells were treated with **2** at 16 μM in 0.2% DMSO, **9** at 10 μM in 0.2% DMSO, **33** at 37 μM in 0.2% DMSO, β-secretase inhibitor IV at 25 μM in 0.2% DMSO, SB216763 at 10 μM in 0.2% DMSO or vehicles alone for 24 h. Concentration of Aβ(1-40)-peptides in culture media was measured using a specific sandwich-type ELISA (*h*Aβ(1–40)

assay kit, IBL, 27718) according to the manufacturer's protocols. Absorbance was read using a

plate reader at 450 nm.

Primary cell cultures (nitrites measurement). Astrocytes were prepared from neonatal (P2) rat

cerebral cortex, as previously described by Luna-Medina et al.[62] All procedures with animals

were specifically approved by the Ethics Committee for Animal Experimentation of the CSIC

and carried out in accordance with National (normative 1201/2005) and International

recommendations (Directive 2010/63 from the European Communities Council). Special care

was taken to minimize animal suffering.

After removal of the meninges, the cerebral cortex was dissected, dissociated, and incubated with

0.25% trypsin/EDTA at 37 °C for 1 h. After centrifugation, the pellet was washed 3 times with

Hank's balanced salt solution (HBSS) (Gibco) and the cells were placed on noncoated flasks and

maintained in HAMS/Dulbecco's modified eagle's medium (DMEM) (1:1) medium containing

10% of FBS. After 15 days, the flasks were agitated on an orbital shaker for 4 h at 240 rpm at 37

°C, the supernatant was collected, centrifuged, and the cellular pellet containing the microglial

cells resuspended in complete medium (HAMS/DMEM (1:1) containing 10% FBS) and seeded

on uncoated 96-well plates. Cells were allowed to adhere for 2 h, and the medium was removed

to eliminate non adherent oligodendrocytes. New fresh medium containing 10 ng/mL of

granulocyte-macrophage colony-stimulating factor (GM-CSF) was added. The remaining

astroglial cells adhered on the flasks were then trypsinized, collected, centrifuged, and plated

onto 96-well plates with complete medium. The purity of cultures obtained by this procedure

was > 98% as determined by immunofluorescence with the OX42 (microglial marker) and the

glial fibrillary acidic protein (GFAP, astroglial marker) antibodies.

Nitrites Measurement. Primary cultures of astrocytes and microglia were incubated with compounds **2**, **9** and **33** at 10 μM for 1 h, and then cultured for another 24 h with LPS (10 μg/mL). Accumulation of nitrites in media was assayed by the standard Griess reaction. Supernatants were collected from the media and mixed with an equal volume of Griess reagent (Sigma-Aldrich). Samples were then incubated at rt for 15 min and absorbance was read using a plate reader at 492/540 nm.

Primary cell cultures (western blot analysis). Mixed glial cell cultures were prepared from cerebral cortex of newborn Wistar rats (*Rattus norvegicus*), as previously described.[63] All animal experiments were authorized by the University of Bologna bioethical committee (Protocol n° 17-72-1212) and performed according to Italian and European Community laws on animal use for experimental purposes. Briefly, brain tissue was cleaned from meninges, trypsinized for 15 min at 37 °C and, after mechanical dissociation, the cell suspension was washed and plated on poly-L-lysine (Sigma-Aldrich, St. Louis, MO, USA, 10 μg/mL) coated flasks (75 cm^2). Mixed glial cells were cultured for 10-13 days in Basal Medium Eagle (BME, Life technologies Ltd, Paisley, UK) supplemented with 100 mL/L heat-inactivated FBS (Life technologies), 2 mmol/L glutamine (Sigma-Aldrich) and 100 μmol/L gentamicin sulphate (Sigma-Aldrich).

Microglial cells were harvested from mixed glial cells cultures by mechanical shaking, resuspended in fresh medium without serum and plated on uncoated 35 mm Ø dishes at a density of 1.5×10^6 cells/1.5 mL medium/well for western blot analysis or on 96 wells at 1×10^5 cells/0.2 mL medium/well for MTT assay. Cells were allowed to adhere for 30 min and then washed to remove non-adhering cells. These primary cultures are pure microglial cells, being

more than 99% of adherent cells positive for isolectin B4 and negative for astrocytes and oligodendrocytes markers.

For the preparation of purified astrocyte cultures, 10-day-old primary mixed glial cultures were vigorously shaken to detach microglia and oligodendrocytes growing on top of the astrocytic layer. The remaining adherent cells were detached with trypsin (0.25%)/EDTA (Life technologies), and the resulting cell suspension was left at room temperature in uncoated flasks to allow adherence of microglia to the plastic surface. After 20-30 min, non-adherent or loosely adherent cells were collected after mild shaking of the flasks, and the adhesion step was performed once more. Supernatants containing non-adherent cells were collected and centrifuged; cells were resuspended in fresh BME medium without serum (Life technologies) and reseeded on poly-L-lysine-coated (Sigma-Aldrich) 35 mm Ø dishes at a density of 1.5×10^6 cells/1.5 mL medium/well for western blot analysis or on 96 wells at 1×105 cells/0.2 mL medium/well for MTT assay. Afterwards, different treatments were performed.

Western blot analysis. Microglial and astrocyte cells exposed to LPS (100 ng/mL) in presence or absence of different concentrations of **2** and **33** (0, 5, 10 and 20 μM) for 24 h were directly in ice-cold lysis buffer (Tris 50 mM, SDS 1 %, protease inhibitor cocktail 0.05%) and protein content was determined by using the Lowry method.[64] 20 μg of protein extracts were resuspended in 20 μL of loading buffer (0.05M Tris-HCl pH 6.8; 40 g/L sodium dodecyl sulfate; 20 mL/L glycerol; 2 g/L bromophenol blue and 0.02 M dithiothreitol; all chemicals were from Sigma-Aldrich) and loaded onto 10% sodium dodecyl sulfate-polyacrylamide gels (SDS-PAGE; Bio-Rad Laboratories SrL, Segrate, MI, IT). After electrophoresis and transfer onto nitrocellulose membranes (GE Healthcare Europe GmbH, Milano, MI, IT), membranes were

blocked for 1 h in 5% non-fat milk (Bio-Rad)/0.1% Tween-20 in phosphate buffered saline (PBS, Sigma-Aldrich), pH 7.4, and incubated overnight) at 4 °C with primary antibodies (rabbit polyclonal anti-iNOS or anti-TREM2 1:1000, both from Santa Cruz Biotechnology Inc., Santa Cruz, CA, USA, or mouse monoclonal anti-βactin, 1:2000, Sigma-Aldrich) in 0.1% Tween-20/PBS. Membranes were then incubated with an anti-rabbit or anti-mouse secondary antibody conjugated to horseradish peroxidase (1:2000; Santa Cruz), for 90 min at rt in 0.1% Tween-20/PBS. Labelled proteins were detected by using the enhanced chemiluminescence method (ECL; Bio-RAD). Densitometric analysis was performed by using Scion Image software from NIH.

NS cultures. NS cultures were derived from the hippocampus of adult rats and induced to proliferate using established passaging methods to achieve optimal cellular expansion according to published protocols.[65] All procedures with animals were specifically approved by the Ethics Committee for Animal Experimentation of the CSIC and carried out in accordance with National (normative 1201/2005) and International recommendations (Directive 2010/63 from the European Communities Council). Special care was taken to minimize animal suffering.

Rats were decapitated, brains removed, and the hippocampus dissected as described.[66] Briefly, cells were seeded into 12-well dishes and cultured in DMEM/F12 (1:1, Invitrogen) containing 10 ng/mL epidermal growth factor (EGF, Peprotech, London, UK), 10 ng/mL fibroblast growth factor (FGF, Peprotech), and B27 medium (Gibco). After 3 days in culture, NS were cultivated in the presence or absence of **2**, **9**, and **33** at 10 μM during a week. After that, NS from 10-day old cultures were plated for 72 h onto 100 μg/mL poly-L-lysine-coated coverslips in the absence of exogenous growth factors.

Immunocytochemistry. Cells were processed for immunocytochemistry to detect neural markers, such as β-tubulin and MAP-2, as previously described.[66] Briefly, at the end of the treatment period, NS cultures were grown on glass coverslips in 24-well cell culture plates. Cultures were then washed with PBS and fixed for 30 min with 4% paraformaldehyde at 25 °C and permeabilized with 0.1% Triton X-100 for 30 min at 37 °C. After 1 h incubation with the selected primary antibodies (polyclonal anti-β-tubulin (clone Tuj1; Abcam) and mouse monoclonal anti-MAP-2 (Sigma-Aldrich)) cells were washed with phosphate-buffered saline and incubated with the corresponding Alexa-labelled secondary antibody (green Alexa-488 and red Alex-647 to reveal β-tubulin and MAP-2, respectively; Molecular Probes; Leiden, The Netherlands) for 45 min at 37 °C. Later on, images were obtained using a TCS SP5 laser scanning spectral confocal microscope (Leica Microsystems). Confocal microscope settings were adjusted to produce the optimum signal-to-noise ratio. Dapi staining was used as a nuclear marker.

Pharmacokinetic studies. Compounds administration. Compound **2** was intraperitoneally administered to CD1 mice at 10 mg/kg dose.

All procedures were approved by Istituto Italiano di Tecnologia licensing, the Italian Ministry of Health and EU guidelines (Directive 2010/63/EU).

Vehicle was: PEG400/Tween 80/saline solution at 10/10/80 % in volume respectively. Three animals per dose were treated. Control animals treated with vehicle only were also included in the experimental protocol. Animals were sacrificed at time-points and blood and brain samples were collected. Plasma was separated from blood by centrifugation for 15 min at 3500 rpm a 4

°C, collected in a eppendorf tube and frozen (-80 °C). Brain samples were homogenized in RIPA buffer (150 mM NaCl, 1.0% Triton X-100, 0.5% sodium deoxycholate, 0.1% sodium dodecyl sulphate, 50 mM Tris, pH 8.0) and were then split in two aliquots kept at -80 °C until analysis. An aliquot was used for compound brain level evaluations, following the same procedure described below for plasma samples. The second aliquot was kept for protein content evaluation by bicinchoninic acid assay (BCA).

LC-MS/MS analysis. The plasma levels of **2** were monitored on a Xevo TQ UPLC-MS/MS triple quadrupole system (Waters, Milford, MS, USA), using an external calibration curve and an internal standard (warfarin). Details of the analytical method follow.

Chromatography. Column Acquity BEH T3 2.1 × 50 mm, 1,7 μm particle size (Waters, USA). Flow rate was 0.5 mL/min. A was H_2O + formic acid 0.1%; B was MeCN + formic acid 0.1%. After 30 sec at 1%B, a linear gradient from 1 to 100%B in 2 min was applied. After further 30 sec at 100%B, the system was reconditioned at 1%B for 30sec.

Mass Spectrometry. Capillary 3KV, cone 30V, source temperature 130 °C, cone gas 20L/h, desolvation gas 800 L/h, desolvation temperature 450 °C. The following multiple reaction monitoring (MRM) transitions were used to quantify **2** and the I.S. (precursor m/z> fragment m/z, collision energy): 237>114, 12eV and 237>124, 18eV for **2**, and 309>163, 14V and 309>251, 18eV for the I.S.

Sample preparation. After centrifugation (20 min at 6000g, at 4 °C) mouse plasma and brain samples (50 μL) were transferred to 96-well plates and added with 150μL of MeCN spiked with 500 nM I.S. After mixing (3 min) samples were centrifuged at 6000g for 15 min at 4 °C. 50 μL of the supernatant were then diluted in eluent A (1:1) and loaded on column (5 μL).

Calibration curve and quality control samples (QCs). **2** was spiked in PBS solution at pH = 7.4 preparing a calibration curve over the 1 nM – 10 μM range. In order to check the overall process efficiency, at the time of the experiment, three quality controls samples were also prepared spiking blank mouse plasma with **2** to final 20, 200 and 2000 nM concentrations. Calibrators and QCs were crashed with MeCN spiked with the I.S. as described for the plasma samples. Dosing solutions, previously diluted 2000 fold in the neat solvent were also included in the samples and tested. The concentration of QCs (back-calculated from the regression curve) ranged from 80 to 110% of the nominal concentration.

Data analysis. 2 plasma levels Vs time profiles were analyzed using PK solutions excel application (Summit Research Service, USA) to derive the most important pharmacokinetic parameters: AUC, Tmax, Cmax, clearance, half-life and volume of distribution.

Calculation of the total concentration of compound 2 in brain. 2 reaches a maximum concentration in 1 mL of brain homogenate of 1.50 ng/mg$_{protein}$, 30 min after intraperitoneal administration at 10 mg kg^{-1} dose. Assuming the average protein concentration in the same homogenate is 40 mg/mL, the total amount of **2** in 1 mL of homogenate is: 1.50 ng/mg × 40 mg/mL = 60.0 ng. This homogenate was obtained by dissolving half of a mouse brain of 0.4 g of weight in 1 mL of solvent. Accordingly, we can deduce that the total amount of **2** in the whole brain is: 60.0 ng × 2 = 120.0 ng. Assuming an average mouse brain density of 1.04 g/mL,[67] the volume occupied by a brain of 0.4 g of weight is: 0.4 g / 1.04 g/mL = 0.38 mL. Thus, **2** reaches a total cerebral concentration at 30 mins of 49 ng / 0.38 mL = 315 ng/mL, which divided by the compound MW (236.25 Da), corresponds to 1.34 μM.

1
2
3
4
5
6
7
8
9
10
11
12
13
14
15
16
17
18
19
20
21
22
23
24
25
26
27
28
29
30
31
32
33
34
35
36
37
38
39
40
41
42
43
44
45
46
47
48
49
50
51
52
53
54
55
56
57
58
59
60

ASSOCIATED CONTENT

Supporting Information

Additional figures illustrating nitrite production in glia and viability of the different brain cells exposed to compounds **2** and **33**, permeability in the PAMPA-BBB assay for compounds **1-34**, cell viability and relative experimental details. This material is available free of charge via the Internet at http://pubs.acs.org.

X-ray crystallographic data for compound **2** has been deposited at the Cambridge Crystallographic Data Centre as CCDC 0001000228543.

AUTHOR INFORMATION

Corresponding Author

*E-mail: andrea.cavalli@unibo.it. Phone: (+39)051 20 9 9735. Fax: (+39)051 20 9 9734.

* E-mail: marialaura.bolognesi@unibo.it. Phone: (+39)051 20 9 9717. Fax: (+39)051 20 9 9734.

Author Contributions

All authors have given approval to the final version of the manuscript.

Notes

The authors declare the following competing financial interest(s): A patent protecting some of the compounds disclosed in this paper was filed by the following authors: Cavalli A., Prati F., Bottegoni G., Favia D. A., Pizzirani D., Scarpelli R., Bolognesi M. L.

ACKNOWLEDGMENT

ABBREVIATIONS

Aβ, amyloid-β; AcOH, acetic acid; AD, Alzheimer's disease; APP , amyloid precursor protein; BACE-1, β-site APP-cleaving enzyme 1; BBB, blood-brain-barrier; BCA, bicinchoninic acid assay; BME, Basal Medium Eagle; $CDCl_3$, deuterated chloroform; CD_3OD, deuterated methanol; CHAPS, 3-[(3-cholamidopropyl)dimethylammonio]-1-propanesulfonate; CNS, central nervous system; $(COCl)_2$, oxalyl chloride; DCM, dichloromethane; DMEM, Dulbecco's modified eagle's medium; DMSO, dimethyl sulfoxide; DMSO-d_6, deuterated dimethyl sulfoxide; D_2O, deuterated water; EDTA, ethylenediaminetetraacetic acid; EGF, epidermal growth factor, EGTA, ethylene glycol tetraacetic acid; ELISA, enzyme-linked immunoabsorbent assay; ESI, electrospray ionization; Et_3N, triethylamine; Et_2O, diethyl ether; EtOAc, ethyl acetate; EtOH, ethanol; FBS, fetal bovine serum; FGF, fibroblast growth factor; FRET, fluorescence resonance energy transfer; GFAP, glial fibrillary acidic protein; GM-CSF, granulocyte-macrophage colony-stimulating factor; GSK-3β, glycogen-synthase kinase-3β; HBSS, Hank's balanced salt solution; HCl, hydrochloric acid; HEPES, 4-(2-hydroxyethyl)-1-piperazineethanesulfonic acid; H_2O, water; HPLC, high-performance liquid chromatography; H_2SO_4, sulfuric acid; Hz, Hertz; iNOS, inducible nitric oxide synthase; I.S., internal standard; *J*, coupling constants; LE, ligand

efficiency; LiAlH$_4$, lithium aluminium hydride; LPS, lipopolysaccharide; MAP-2, microtubule associated protein 2; MeCN, acetonitrile; MeOH, methanol; MRM, multiple reaction monitoring; MTDLs, multitarget-directed ligands; MTT, 3-(4,5-dimethylthiazol-2-yl)-2,5-diphenyltetrazolium bromide; Na$_2$CO$_3$, sodium carbonate; NaCl, sodium chloride; NaHCO$_3$, sodium bicarbonate; NaOH, sodium hydroxide; Na$_2$SO$_4$, sodium sulfate; NMR, nuclear magnetic resonance; NH$_3$, ammonia; NH$_4$OAc, ammonium acetate; NS, neurosphere; NTF, neurofibrillary tangles; PAMPA, parallel artificial membrane permeability assay; PBS, phosphate buffered saline; PDA, photodiode array detector; ppm, parts per million; *Pe*, permeability; P-τ, phosphorylated τ protein; QCs, quality control samples; ROS, reactive oxygen species; rt, room temperature; SAR, structure-activity relationships; SQD-MS, single quadropole mass spectrometer; THF, tetrahydrofurane; TLC, thin layer chromatography; TREM2, triggering receptor expressed on myeloid cells 2; UPLC-MS, ultra performance liquid chromatography-mass.

REFERENCES

(1) Alzheimer'sAssociation. (2014) Alzheimer's Association Report 2014 Alzheimer's disease facts and figures, *Alzheimer's & Dementia 10*, e47-e92.

(2) Pangalos, M. N., Schechter, L. E., and Hurko, O. (2007) Drug development for CNS disorders: strategies for balancing risk and reducing attrition, *Nat. Rev. Drug Discov. 6*, 521-532.

(3) Cummings, J. L., Morstorf, T., and Zhong, K. (2014) Alzheimer's disease drug-development pipeline: few candidates, frequent failures, *Alzheimers Res. Ther. 6*, 37.

(4) Iqbal, K., and Grundke-Iqbal, I. (2010) Alzheimer's disease, a multifactorial disorder seeking multitherapies, *Alzheimers Dement. 6*, 420-424.

(5) Palop, J. J., Chin, J., and Mucke, L. (2006) A network dysfunction perspective on neurodegenerative diseases, *Nature 443*, 768-773.

(6) Morphy, R., and Rankovic, Z. (2005) Designed multiple ligands. An emerging drug discovery paradigm, *J. Med. Chem. 48*, 6523-6543.

(7) Hopkins, A. L. (2008) Network pharmacology: the next paradigm in drug discovery, *Nat. Chem. Biol. 4*, 682-690.

(8) Cavalli, A., Bolognesi, M. L., Minarini, A., Rosini, M., Tumiatti, V., Recanatini, M., and Melchiorre, C. (2008) Multi-target-directed ligands to combat neurodegenerative diseases, *J. Med. Chem. 51*, 347-372.

(9) Prati, F., Uliassi, E., and Bolognesi, M. L. (2014) Two diseases, one approach: multitarget drug discovery in Alzheimer's and neglected tropical diseases, *Medchemcomm 5*, 853-861.

(10) Geldenhuys, W. J., Youdim, M. B., Carroll, R. T., and Van der Schyf, C. J. (2011) The emergence of designed multiple ligands for neurodegenerative disorders, *Prog. Neurobiol. 94*, 347-359.

(11) Dunkel, P., Chai, C. L., Sperlagh, B., Huleatt, P. B., and Matyus, P. (2012) Clinical utility of neuroprotective agents in neurodegenerative diseases: current status of drug development for Alzheimer's, Parkinson's and Huntington's diseases, and amyotrophic lateral sclerosis, *Expert. Opin. Investig. Drugs 21*, 1267-1308.

(12) Viayna, E., Sabate, R., and Munoz-Torrero, D. (2013) Dual inhibitors of beta-amyloid aggregation and acetylcholinesterase as multi-target anti-Alzheimer drug candidates, *Curr. Top. Med. Chem. 13*, 1820-1842.

(13) Leon, R., Garcia, A. G., and Marco-Contelles, J. (2013) Recent advances in the multitarget-directed ligands approach for the treatment of Alzheimer's disease, *Med. Res. Rev. 33*, 139-189.

(14) Chen, X., and Decker, M. (2013) Multi-target compounds acting in the central nervous system designed from natural products, *Curr. Med. Chem. 20*, 1673-1685.

(15) Zheng, H., Fridkin, M., and Youdim, M. (2015) New approaches to treating Alzheimer's disease, *Perspect Medicin Chem 7*, 1-8.

(16) (2012) *Polypharmacology in Drug Discovery*, John Wiley & Sons, Inc., Hoboken, New Jersey.

(17) Vassar, R., and Citron, M. (2000) Abeta-generating enzymes: recent advances in beta- and gamma-secretase research, *Neuron 27*, 419-422.

(18) Avila, J., Wandosell, F., and Hernandez, F. (2010) Role of glycogen synthase kinase-3 in Alzheimer's disease pathogenesis and glycogen synthase kinase-3 inhibitors, *Expert. Rev. Neurother. 10*, 703-710.

(19) Hardy, J., and Selkoe, D. J. (2002) The amyloid hypothesis of Alzheimer's disease: progress and problems on the road to therapeutics, *Science 297*, 353-356.

(20) Grundke-Iqbal, I., Iqbal, K., Quinlan, M., Tung, Y. C., Zaidi, M. S., and Wisniewski, H. M. (1986) Microtubule-associated protein tau. A component of Alzheimer paired helical filaments, *J. Biol. Chem. 261*, 6084-6089.

(21) Llorens-Martin, M., Jurado, J., Hernandez, F., and Avila, J. (2014) GSK-3beta, a pivotal kinase in Alzheimer disease, *Front. Mol. Neurosci. 7*, 46.

(22) Prati, F., De Simone, A., Bisignano, P., Armirotti, A., Summa, M., Pizzirani, D., Scarpelli, R., Perez, D. I., Andrisano, V., Perez-Castillo, A., Monti, B., Massenzio, F., Polito, L., Racchi, M., Favia, A. D., Bottegoni, G., Martinez, A., Bolognesi, M. L., and Cavalli, A. (2015) Multitarget Drug Discovery for Alzheimer's Disease: Triazinones as BACE-1 and GSK-3beta Inhibitors, *Angew. Chem. Int. Ed. Engl. 54*, 1578-1582.

(23) Bottegoni, G., Favia, A. D., Recanatini, M., and Cavalli, A. (2012) The role of fragment-based and computational methods in polypharmacology, *Drug. Discov. Today 17*, 23-34.

(24) Hopkins, A. L., Mason, J. S., and Overington, J. P. (2006) Can we rationally design promiscuous drugs?, *Curr. Opin. Struct. Biol. 16*, 127-136.

(25) Yuan, J., Venkatraman, S., Zheng, Y., McKeever, B. M., Dillard, L. W., and Singh, S. B. (2013) Structure-based design of beta-site APP cleaving enzyme 1 (BACE1) inhibitors for the treatment of Alzheimer's disease, *J. Med. Chem. 56*, 4156-4180.

(26) Ghosh, A. K., and Osswald, H. L. (2014) BACE1 (beta-secretase) inhibitors for the treatment of Alzheimer's disease, *Chem. Soc. Rev. 43*, 6765-6813.

(27) Kramer, T., Schmidt, B., and Lo Monte, F. (2012) Small-Molecule Inhibitors of GSK-3: Structural Insights and Their Application to Alzheimer's Disease Models, *Int. J. Alzheimers Dis. 2012*, 381029.

(28) Ghose, A. K., Herbertz, T., Hudkins, R. L., Dorsey, B. D., and Mallamo, J. P. (2012) Knowledge-Based, Central Nervous System (CNS) Lead Selection and Lead Optimization for CNS Drug Discovery, *ACS Chem. Neurosci. 3*, 50-68.

(29) Ostrogovich, A. (1909) Sopra alcuni nuovi derivati della guanilurea *Gazz. Chim. It. 39*, 540-549.

(30) McLure, K. G., and Young, P. R. (2013) Preparation of substituted 2-phenyl-3Hquinazolin-4-ones and analogs as inhibitors of BET for treating cancer.

(31) Nangia, A. (2008) Conformational polymorphism in organic crystals, *Accounts Chem.Res. 41*, 595-604.

(32) Morphy, R., and Rankovic, Z. (2007) Fragments, network biology and designing multiple ligands, *Drug Discov. Today 12*, 156-160.

(33) Perez-Areales, F. J., Di Pietro, O., Espargaro, A., Vallverdu-Queralt, A., Galdeano, C., Ragusa, I. M., Viayna, E., Guillou, C., Clos, M. V., Perez, B., Sabate, R., Lamuela-Raventos, R. M., Luque, F. J., and Munoz-Torrero, D. (2014) Shogaol-huprine hybrids: dual antioxidant and anticholinesterase agents with beta-amyloid and tau anti-aggregating properties, *Bioorg. Med. Chem. 22*, 5298-5307.

(34) Mariano, M., Schmitt, C., Miralinaghi, P., Catto, M., Hartmann, R. W., Carotti, A., and Engel, M. (2014) First selective dual inhibitors of tau phosphorylation and Beta-amyloid aggregation, two major pathogenic mechanisms in Alzheimer's disease, *ACS Chem. Neurosci. 5*, 1198-1202.

(35) Mancini, F., De Simone, A., and Andrisano, V. (2011) Beta-secretase as a target for Alzheimer's disease drug discovery: an overview of in vitro methods for characterization of inhibitors, *Anal. Bioanal. Chem. 400*, 1979-1996.

(36) Baki, A., Bielik, A., Molnar, L., Szendrei, G., and Keseru, G. M. (2007) A high throughput luminescent assay for glycogen synthase kinase-3beta inhibitors, *Assay Drug Dev. Technol. 5*, 75-83.

(37) Hopkins, A. L., Keseru, G. M., Leeson, P. D., Rees, D. C., and Reynolds, C. H. (2014) The role of ligand efficiency metrics in drug discovery, *Nat. Rev. Drug Discov. 13*, 105-121.

(38) Beurel, E., Michalek, S. M., and Jope, R. S. (2010) Innate and adaptive immune responses regulated by glycogen synthase kinase-3 (GSK3), *Trends Immunol. 31*, 24-31.

(39) Boche, D., Perry, V. H., and Nicoll, J. A. (2013) Review: activation patterns of microglia and their identification in the human brain, *Neuropathol. Appl. Neurobiol. 39*, 3-18.

(40) Goldmann, T., and Prinz, M. (2013) Role of microglia in CNS autoimmunity, *Clin. Dev. Immunol. 2013*, 208093.

(41) Contestabile, A., Monti, B., and Polazzi, E. (2012) Neuronal-glial Interactions Define the Role of Nitric Oxide in Neural Functional Processes, *Curr. Neuropharmacol. 10*, 303-310.

(42) Rohn, T. T. (2013) The triggering receptor expressed on myeloid cells 2: "TREM-ming" the inflammatory component associated with Alzheimer's disease, *Oxid. Med. Cell. Longev. 2013*, 860959.

(43) Lange, C., Mix, E., Frahm, J., Glass, A., Muller, J., Schmitt, O., Schmole, A. C., Klemm, K., Ortinau, S., Hubner, R., Frech, M. J., Wree, A., and Rolfs, A. (2011) Small molecule GSK-3 inhibitors increase neurogenesis of human neural progenitor cells, *Neurosci. Lett. 488*, 36-40.

(44) Morales-Garcia, J. A., Luna-Medina, R., Alonso-Gil, S., Sanz-SanCristobal, M., Palomo, V., Gil, C., Santos, A., Martinez, A., and Perez-Castillo, A. (2012) Glycogen Synthase Kinase 3 Inhibition Promotes Adult Hippocampal Neurogenesis in Vitro and in Vivo, *ACS Chem. Neurosci. 3*, 963-971.

(45) Pardridge, W. M. (2005) The blood-brain barrier: bottleneck in brain drug development, *NeuroRx 2*, 3-14.

(46) Di, L., Kerns, E. H., Fan, K., McConnell, O. J., and Carter, G. T. (2003) High throughput artificial membrane permeability assay for blood-brain barrier, *Eur. J. Med. Chem. 38*, 223-232.

(47) Crivori, P., Cruciani, G., Carrupt, P. A., and Testa, B. (2000) Predicting blood-brain barrier permeation from three-dimensional molecular structure, *J. Med. Chem. 43*, 2204-2216.

(48) Tachikawa, M., and Hosoya, K. (2011) Transport characteristics of guanidino compounds at the blood-brain barrier and blood-cerebrospinal fluid barrier: relevance to neural disorders, *Fluids Barriers CNS 8*, 13.

(49) McConlogue, L., Buttini, M., Anderson, J. P., Brigham, E. F., Chen, K. S., Freedman, S. B., Games, D., Johnson-Wood, K., Lee, M., Zeller, M., Liu, W., Motter, R., and Sinha, S. (2007) Partial reduction of BACE1 has dramatic effects on Alzheimer plaque and synaptic pathology in APP transgenic mice, *J. Biol. Chem. 282*, 26326-26334.

(50) Avrahami, L., Licht-Murava, A., Eisenstein, M., and Eldar-Finkelman, H. (2013) GSK-3 inhibition: achieving moderate efficacy with high selectivity, *Biochim. Biophys. Acta 1834*, 1410-1414.

(51) Martinez, A., Perez, D. I., and Gil, C. (2013) Lessons learnt from glycogen synthase kinase 3 inhibitors development for Alzheimer's disease, *Curr. Top. Med. Chem. 13*, 1808-1819.

(52) Zheng, H., Fridkin, M., and Youdim, M. (2014) From single target to multitarget/network therapeutics in Alzheimer's therapy, *Pharmaceuticals (Basel) 7*, 113-135.

(53) Terwel, D., Muyllaert, D., Dewachter, I., Borghgraef, P., Croes, S., Devijver, H., and Van Leuven, F. (2008) Amyloid activates GSK-3beta to aggravate neuronal tauopathy in bigenic mice, *Am. J. Pathol. 172*, 786-798.

(54) Zhang, H., Ma, Q., Zhang, Y. W., and Xu, H. (2012) Proteolytic processing of Alzheimer's beta-amyloid precursor protein, *J. Neurochem. 120 Suppl 1*, 9-21.

(55) Uemura, K., Kuzuya, A., Shimozono, Y., Aoyagi, N., Ando, K., Shimohama, S., and Kinoshita, A. (2007) GSK3beta activity modifies the localization and function of presenilin 1, *J. Biol. Chem. 282*, 15823-15832.

(56) Ly, P. T., Wu, Y., Zou, H., Wang, R., Zhou, W., Kinoshita, A., Zhang, M., Yang, Y., Cai, F., Woodgett, J., and Song, W. (2013) Inhibition of GSK3beta-mediated BACE1 expression reduces Alzheimer-associated phenotypes, *J. Clin. Invest. 123*, 224-235.

(57) Duisenberg, A. J. M., Hooft, R. W. W., Schreurs, A. M. M., and Kroon, J. (2000) Accurate cells from area-detector images, *J. Appl. Crystallogr. 33*, 893-898.

(58) Duisenberg, A. J. M. (1992) Indexing in Single-Crystal Diffractometry with an Obstinate List of Reflections, *J. Appl. Crystallogr. 25*, 92-96.

(59) Farrugia, L. J. (1999) WinGX suite for small-molecule single-crystal crystallography, *J. Appl. Crystallogr. 32*, 837-838.

(60) Farrugia, L. J. (1997) ORTEP-3 for Windows - a version of ORTEP-III with a Graphical User Interface (GUI), *J. Appl. Crystallogr. 30*, 565.

(61) Coghlan, M. P., Culbert, A. A., Cross, D. A., Corcoran, S. L., Yates, J. W., Pearce, N. J., Rausch, O. L., Murphy, G. J., Carter, P. S., Roxbee Cox, L., Mills, D., Brown, M. J., Haigh, D., Ward, R. W., Smith, D. G., Murray, K. J., Reith, A. D., and Holder, J. C. (2000) Selective small molecule inhibitors of glycogen synthase kinase-3 modulate glycogen metabolism and gene transcription, *Chem. Biol. 7*, 793-803.

(62) Luna-Medina, R., Cortes-Canteli, M., Alonso, M., Santos, A., Martinez, A., and Perez-Castillo, A. (2005) Regulation of inflammatory response in neural cells in vitro by thiadiazolidinones derivatives through peroxisome proliferator-activated receptor gamma activation, *J. Biol. Chem. 280*, 21453-21462.

(63) Monti, B., D'Alessandro, C., Farini, V., Bolognesi, A., Polazzi, E., Contestabile, A., Stirpe, F., and Battelli, M. G. (2007) In vitro and in vivo toxicity of type 2 ribosome-inactivating proteins lanceolin and stenodactylin on glial and neuronal cells, *Neurotoxicology 28*, 637-644.

(64) Lowry, O. H., Rosebrough, N. J., Farr, A. L., and Randall, R. J. (1951) Protein measurement with the Folin phenol reagent, *J. Biol. Chem. 193*, 265-275.

(65) Ferron, S. R., Andreu-Agullo, C., Mira, H., Sanchez, P., Marques-Torrejon, M. A., and Farinas, I. (2007) A combined ex/in vivo assay to detect effects of exogenously added factors in neural stem cells, *Nat. Protoc. 2*, 849-859.

(66) Morales-Garcia, J. A., Luna-Medina, R., Alfaro-Cervello, C., Cortes-Canteli, M., Santos, A., Garcia-Verdugo, J. M., and Perez-Castillo, A. (2011) Peroxisome proliferator-activated receptor gamma ligands regulate neural stem cell proliferation and differentiation in vitro and in vivo, *Glia 59*, 293-307.

(67) Bothe, H. W., Bodsch, W., and Hossmann, K. A. (1984) Relationship between specific gravity, water content, and serum protein extravasation in various types of vasogenic brain edema, *Acta Neuropathol. 64*, 37-42.

Table 1. Inhibitory potencies (IC$_{50}$) of compounds **1-34** and reference compounds inhibitor IV
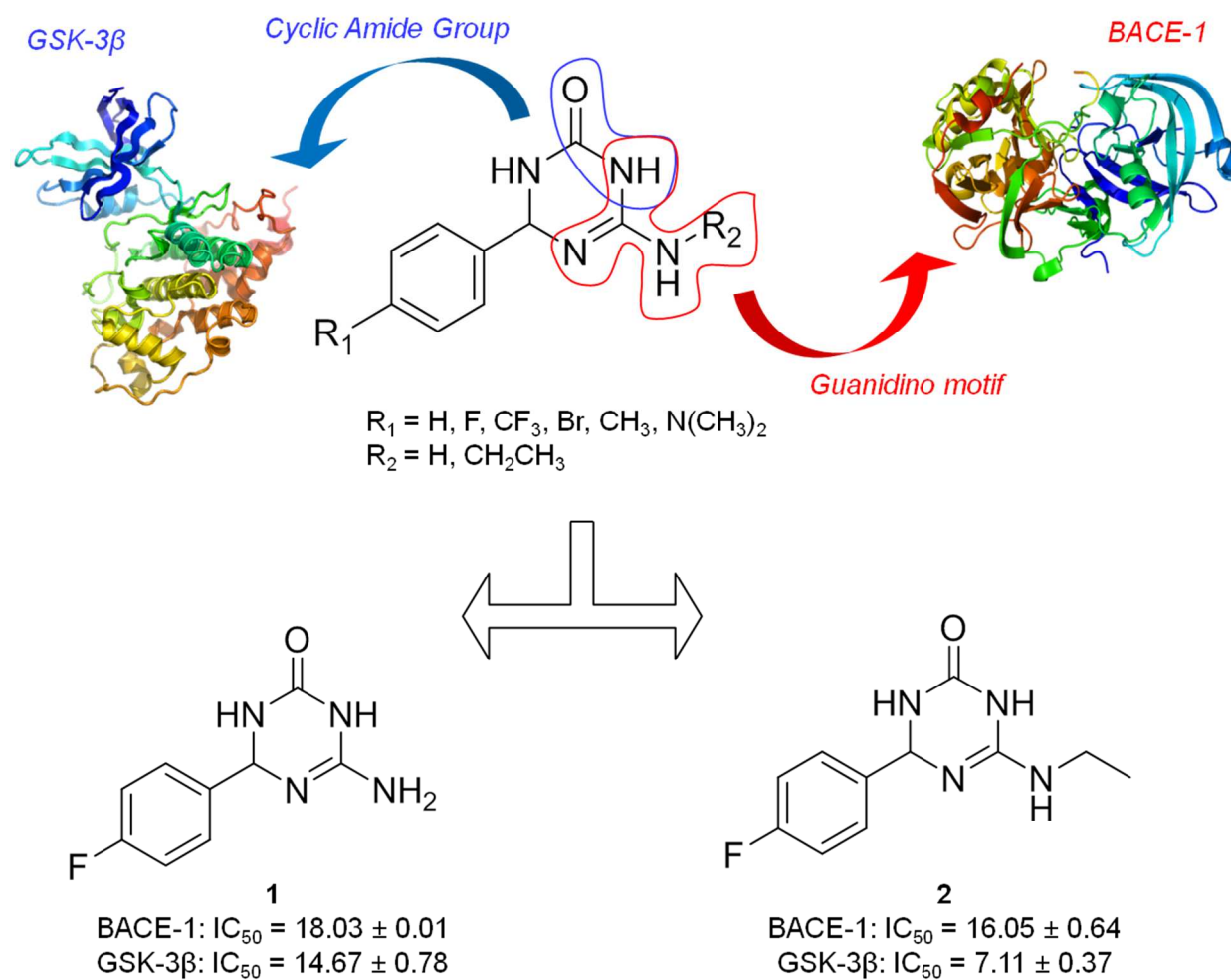and SB415286 against BACE-1 and GSK-3β, respectively.

Comp	Structure	BACE-1 IC$_{50}$ (μM)^a ± S.E.M.	GSK-3β IC$_{50}$ (μM)^a ± S.E.M.
1	X = O, R$_1$ = H, Ar = 4-F-Ph	18.03 ± 0.01^b	14.67 ± 0.78^b
2	X = O, R$_1$ = Et, Ar = 4-F-Ph; R= CH$_2$CH$_3$	16.05 ± 0.64^b	7.11 ± 0.37^b
3	X = O, R$_1$ = H, Ar = 2-NO$_2$-Ph	n.a	24.65 ± 0.20
4	X = O, R$_1$ = H, Ar = 3-NO$_2$-Ph	n.a	25.21 ± 0.15
5	X = O, R$_1$ = H, Ar = 4-NO$_2$-Ph	n.d.	n.d.
6	X = O, R$_1$ = H, Ar = 2-Br-Ph	38.50 ± 0.48	23.51 ± 1.02
7	X = O, R$_1$ = H, Ar = 3-Br-Ph	46.01 ± 0.94	21.14 ± 3.75
8	X = O, R$_1$ = H, Ar = 2-F-Ph	63.14 ± 1.34	10.58 ± 0.01
9	X = O, R$_1$ = H, Ar = 3-F-Ph	10.18 ± 1.02	32.41 ± 4.76
10	X = O, R$_1$ = H, Ar = 2-CF$_3$-Ph	45.03 ± 4.74	16.36 ± 3.33
11	X = O, R$_1$ = H, Ar = 3-CF$_3$-Ph	42.15 ± 7.89	52.13 ± 0.24
12	X = O, R$_1$ = H, Ar = 2-Cl-Ph	84.72 ± 31.62	36.18 ± 2.19
13	X = O, R$_1$ = H, Ar = 3-Cl-Ph	45.33 ± 14.93	13.28 ± 3.64
14	X = O, R$_1$ = H, Ar = 4-Cl-Ph	26.26 ± 4.08	18.03 ± 5.59
15	X = O, R$_1$ = H, Ar = 2-CH$_3$-Ph	198.74 ± 0.04	10.73 ± 0.16
16	X = O, R$_1$ = H, Ar = 3-CH$_3$-Ph	108.9 ± 53.09	16.41 ± 4.39
17	X = O, R$_1$ = H, Ar = 3-N(CH$_3$)$_2$-Ph	431.33 ± 217.62	11.63 ± 4.64
18	X = O, R$_1$ = H, Ar = 4-((diethylamino)methyl)Ph	n.d.	559.32 ± 58.13.
19	X = O, R$_1$ = H, Ar = 4-((morpholino)methyl)Ph	n.a.	31.84 ± 10.73
20	X = O, R$_1$ = H, Ar = 4-((piperidino)methyl)Ph	n.a.	57.65 ± 12.58
21	X = O, R$_1$ = H, Ar = 4-((*N*-methylpiperazino)methyl)Ph	n.a.	163.98 ± 35.78
22	X = O, R$_1$ = H, Ar = 4-Ph-Ph	n.d.	n.d.
23	X = O, R$_1$ = H, Ar = 3,4-dichloro-Ph	49.01 ± 0.03	10.14 ± 0.04
24	X = O, R$_1$ = H, Ar = 3,5-difluoro-Ph	18.21 ± 1.36	21.15 ± 0.59
25	X = O, R$_1$ = H, Ar = 4,5-dihydrobenzo[*c*][1,4]dioxine	n.d.	n.d.
26	X = O, R$_1$ = H, Ar = 3-pyridinyl	39.59 ± 0.85	13.89 ± 0.95
27	X = O, R$_1$ = H, Ar = 4-pyridinyl	n.a.	21.68 ± 6.13
28	X = S, R$_1$ = H, Ar = Ph	43.15 ± 15.42	39.00 ± 9.32
29	X = S, R$_1$ = H, Ar = 2-F-Ph	60.19 ± 16.35	13.78 ± 1.15
30	X = S, R$_1$ = H, Ar = 4-F-Ph	48.88 ± 0.24	14.32 ± 0.01
31	X = S, R$_1$ = H, A r= 2-CH$_3$-Ph	n.d.	n.d.
32	X = O, R$_1$ = CH$_2$CH$_3$, Ar = 2-CH$_3$-Ph	50.31 ± 6.61	40.71 ± 2.70
33	X = O, R$_1$ = (CH$_2$)$_2$CH$_3$, A r = 4-F-Ph	36.83 ± 9.85	4.34 ± 0.63
34	X = O, R$_1$ = Ph, A r= 4-F-Ph	n.a.	6.93 ± 0.14
Inhibitor IV		0.02 ± 0.00	
SB451826			0.05 ± 0.01

^{a}IC$_{50}$ values are reported as a mean value of three or more determinations. ^{b} Data derived from

reference 22. n.a.: not active up to a concentration of 100 μM. n.d.: not determined due to

solubility problems.

Table 2. Pharmacokinetic parameters of **2** after intraperitoneal administration (10 mg kg^{-1}) in mice.

Parameters		**2** IP (10 mg kg^{-1})
C_{max} plasma (obs)	ng mL^{-1}	695
C_{max} brain (obs)	ng mg$_{protein}^{-1}$	1.50
T_{max} (obs)	min	15
AUC(0-t) plasma (obs area)	ng min mL^{-1}	31818
V_d	mL kg^{-1}	72320
CL	mL min^{-1} kg^{-1}	306
$t_{1/2}$	min	163

C_{max} = maximum observed concentration; T_{max} = time corresponding to C_{max}; AUC = cumulative area under curve for experimental time points (0–8 h); Vd = distribution volume; CL = systemic clearance based on observed data points (0–8 h); $t_{1/2}$ = time for concentration to diminish by one-half; F (%) = oral bioavailability.

GSK-3β

Cyclic Amide Group

BACE-1

Guanidino motif

R_1 = H, F, CF_3, Br, CH_3, $N(CH_3)_2$
R_2 = H, CH_2CH_3

1
BACE-1: IC_{50} = 18.03 ± 0.01
GSK-3β: IC_{50} = 14.67 ± 0.78

2
BACE-1: IC_{50} = 16.05 ± 0.64
GSK-3β: IC_{50} = 7.11 ± 0.37
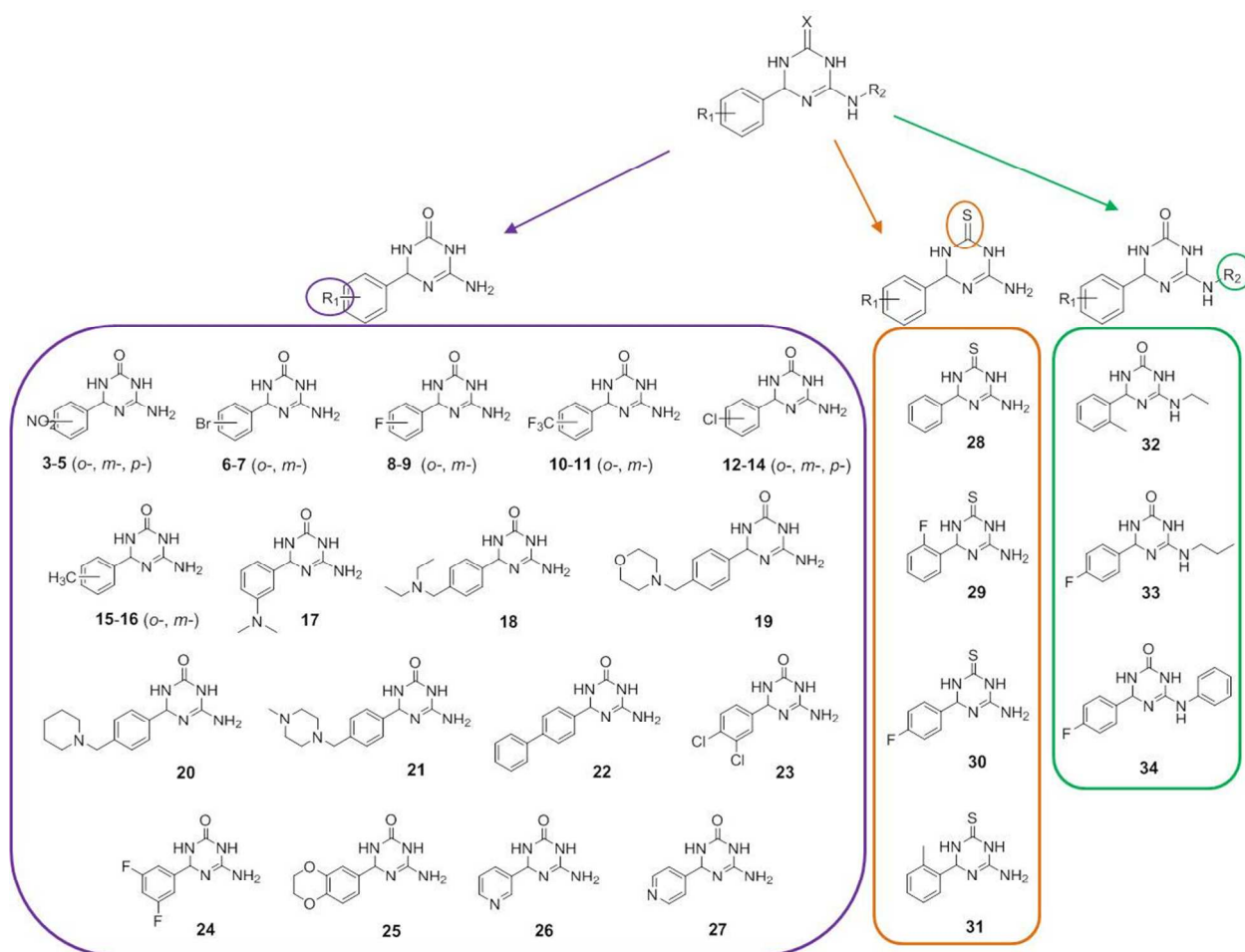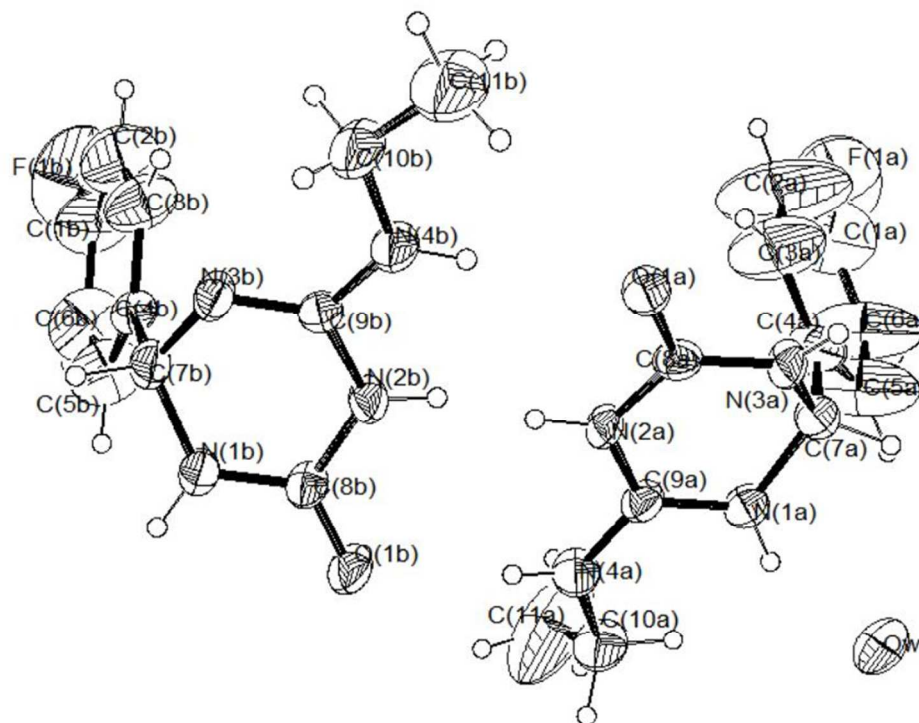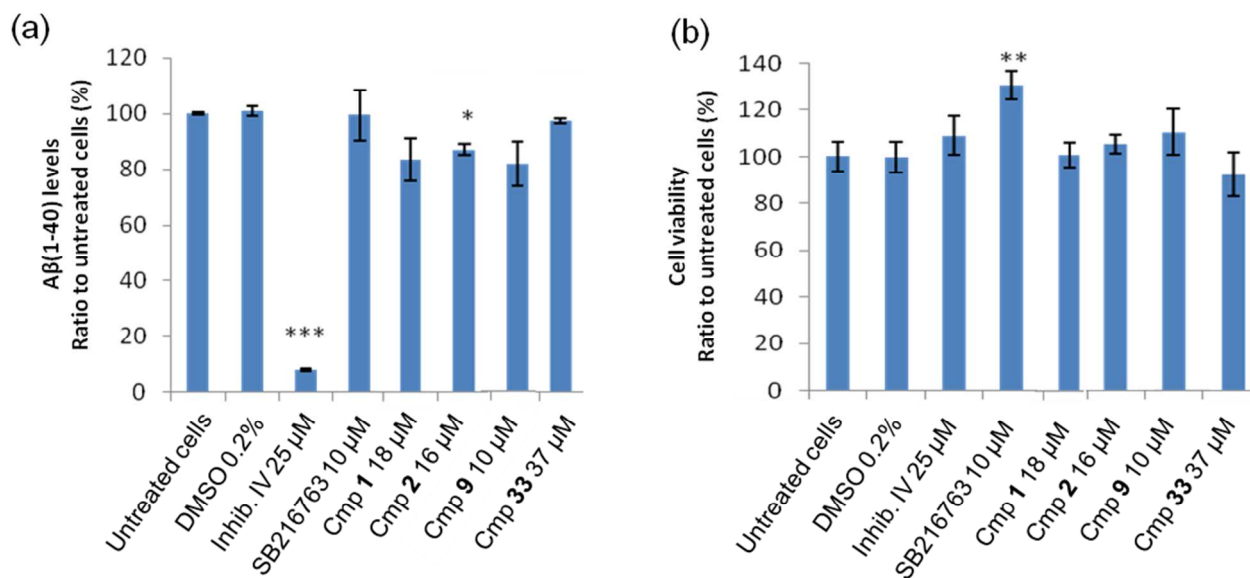
Figure 1. Rational design to hit compounds **1** and **2**.

**Figure 2.** SAR investigation leading to compounds **3-34**.

Figure 3. ORTEP drawing (30% probability) of compound **2**, showing the crystal structure,

together with its crystallographic numbering and main geometrical parameters.
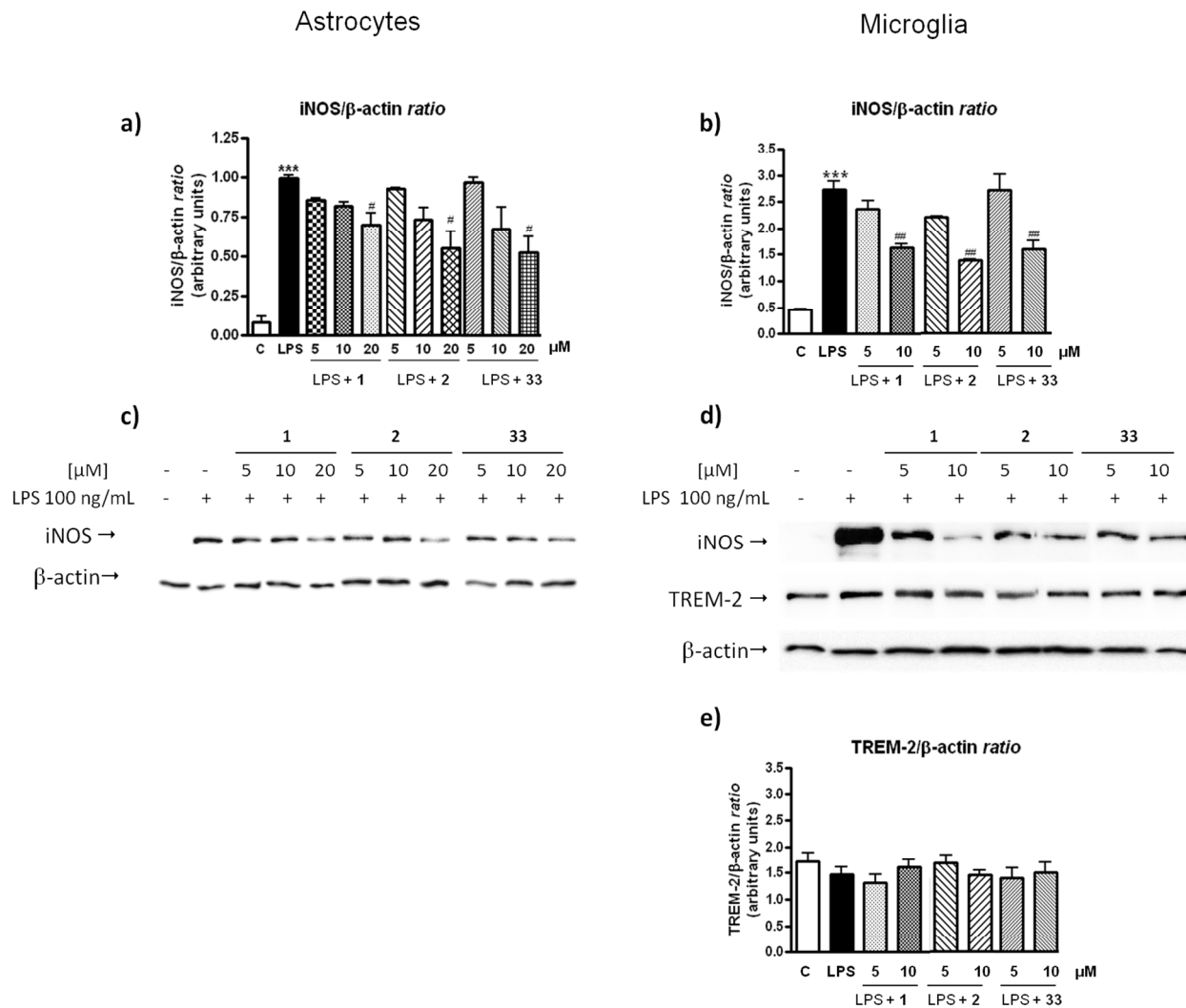
Figure 4. H4-APP$_{sw}$ cells were treated in the presence of selected compounds for 24 h. (a) Aβ(1-40) levels in conditioned media were quantified through enzyme-linked immunosorbent assay (ELISA), and adjusted to take into account differences in cell proliferation. (b) Cell viability was assessed through MTT assay. Each experiment was conducted in triplicate. Data represent mean ± SD. **p<0.01, *p<0.05, *** p<0.001, Student t Test compared to cell treated with vehicle alone.
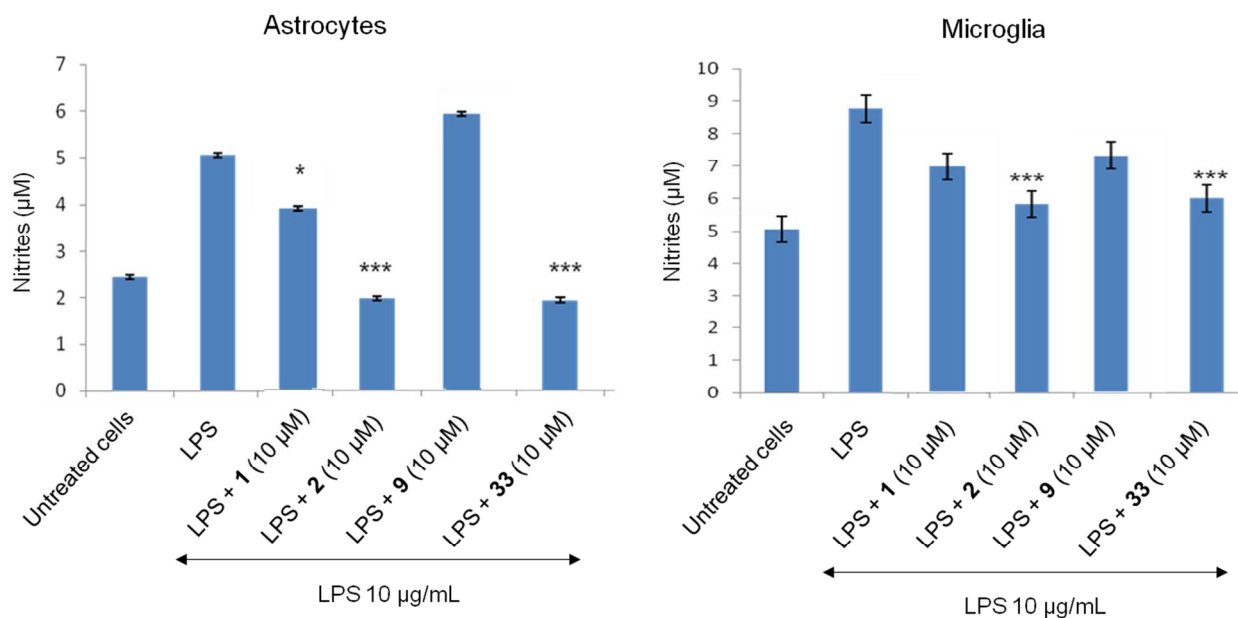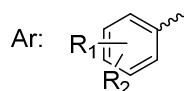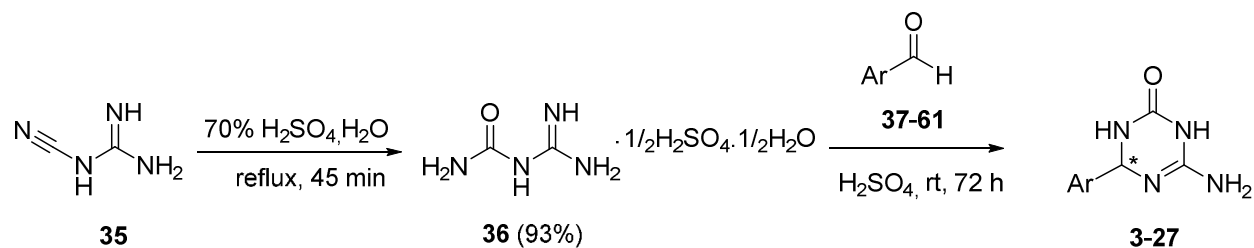
Figure 5. Primary astrocyte and microglial cells were treated with LPS in the absence or presence of **1**, **2**, **9**, and **33**. The production of nitrites from the medium was measured with the Griess reaction.
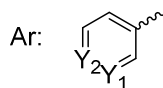
65

Figure 6. Primary rat microglia and astrocyte cells were treated with LPS (100 ng/mL) in the presence or absence of **1**, **2** and **33**. Immunomodulatory activity in glial cells was evaluated through western blot analysis of iNOS (a-d) and TREM2 (d, e) expression, using β-actin as control.
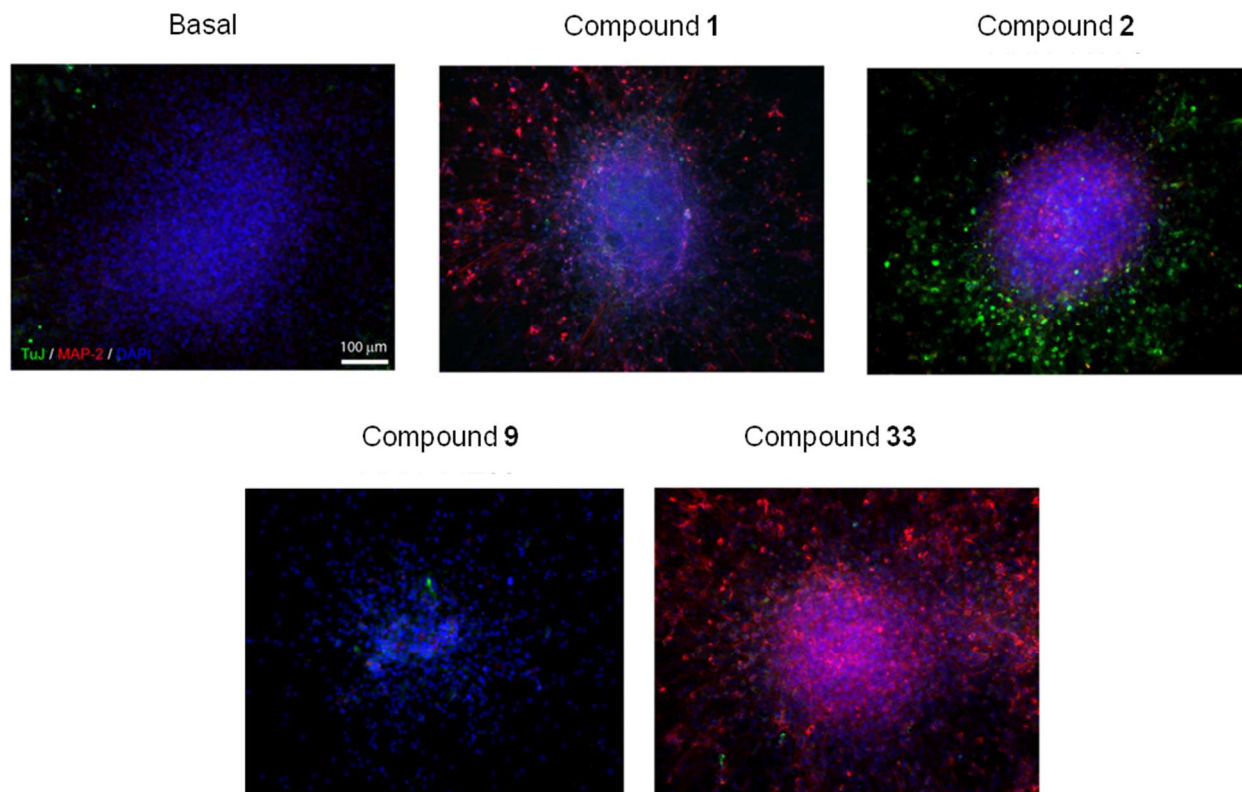
Figure 7. The NSs were cultivated in the absence or presence of **1**, **2**, **9**, and **33** (10 µM) during a week. After that, they were first incubated with anti-β-tubulin and anti-MAP-2 antibodies, and treated with the corresponding Alexa-labelled secondary antibodies (green and red labels to reveal β-tubulin and MAP-2, respectively). DAPI staining (blue) was used as nuclear marker.
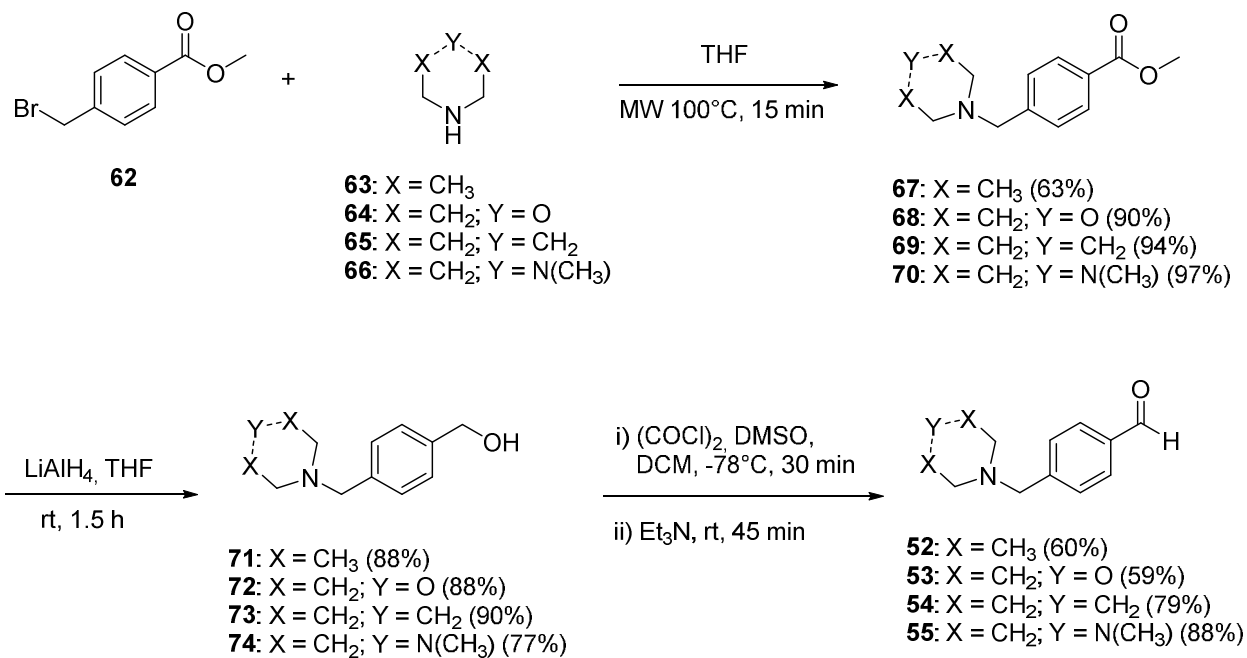
67

1
2
3
4
5
6
7
8
9
10
11
12
13
14
15
16
17
18
19
20
21
22
23
24
25
26
27
28
29
30
31
32
33
34
35
36
37
38
39
40
41
42
43
44
45
46
47
48
49
50
51
52
53
54
55
56
57
58
59
60

Ar:

3: R_1 = H; R_2 = 2-NO_2 (16%)
4: R_1 = H; R_2 = 3-NO_2 (53%)
5: R_1 = H; R_2 = 4-NO_2 (22%)
6: R_1 = H; R_2 = 2-Br (54%)
7: R_1 = H; R_2 = 3-Br (38%)
8: R_1 = H; R_2 = 2-F (62%)
9: R_1 = H; R_2 = 3-F (71%)
10: R_1 = H; R_2 = 2-CF_3 (12%)
11: R_1 = H; R_2 = 3-CF_3 (50%)
12: R_1 = H; R_2 = 2-Cl (64%)
13: R_1 = H; R_2 = 3-Cl (61%)
14: R_1 = H; R_2 = 4-Cl (67%)

15: R_1 = H; R_2 = 2-CH_3 (33%)
16: R_1 = H; R_2 = 3-CH_3 (33%)
17: R_1 = H; R_2 = 3-$N(CH_3)_2$ (48%)
18: R_1 = H; R_2 = 4-(diethylamino)methyl (57%)
19: R_1 = H; R_2 = 4-(morpholino)methyl (61%)
20: R_1 = H; R_2 = 4-(piperidino)methyl (63%)
21: R_1 = H; R_2 = 4-(N-methylpiperazino)methyl (54%)
22: R_1 = H; R_2 = 4-phenyl (26%)
23: R_1 = 3-Cl; R_2 = 4-Cl (80%)
24: R_1 = 3-F; R_2 = 5-F (71%)
25: R_1 = R_2 = [c]-1,4-dioxane (10%)

Ar:

26: Y_1 = N; Y_2 = CH (12%)   **27**: Y_1 =CH; Y_2 = N (12%)

Scheme 1. Synthesis of 6-amino-4-aryl-3,4-dihydro-1,3,5-triazin-2(1*H*)-ones **3-27**.

62

63: X = CH$_3$
64: X = CH$_2$; Y = O
65: X = CH$_2$; Y = CH$_2$
66: X = CH$_2$; Y = N(CH$_3$)

THF
MW 100°C, 15 min

67: X = CH$_3$ (63%)
68: X = CH$_2$; Y = O (90%)
69: X = CH$_2$; Y = CH$_2$ (94%)
70: X = CH$_2$; Y = N(CH$_3$) (97%)

LiAlH$_4$, THF
rt, 1.5 h

71: X = CH$_3$ (88%)
72: X = CH$_2$; Y = O (88%)
73: X = CH$_2$; Y = CH$_2$ (90%)
74: X = CH$_2$; Y = N(CH$_3$) (77%)

i) (COCl)$_2$, DMSO,
   DCM, -78°C, 30 min

ii) Et$_3$N, rt, 45 min

52: X = CH$_3$ (60%)
53: X = CH$_2$; Y = O (59%)
54: X = CH$_2$; Y = CH$_2$ (79%)
55: X = CH$_2$; Y = N(CH$_3$) (88%)

Scheme 2. Synthesis of 4-(aminomethyl)benzaldehydes **52**-**55**.

75

76: R = H
42: R = 2-F
77: R = 4-F
49: R = 2-CH₂

28: R = H (7%)
29: R = 2-F (3%)
30: R = 4-F (3%)
31: R = 2-CH₂ (66%)
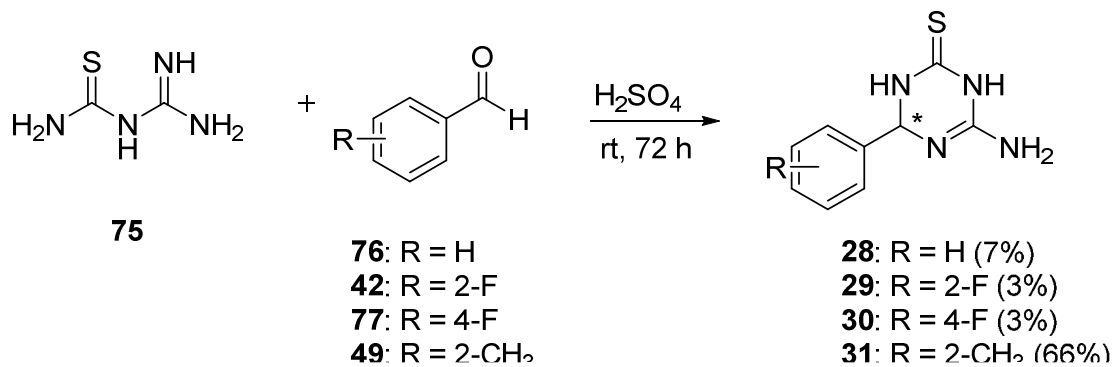
Scheme 3. Synthesis of 6-amino-4-aryl-3,4-dihydro-1,3,5-triazinthiones **28-31**.

81

82: R$_1$ = CH$_2$CH$_3$
83: R$_1$ = (CH$_2$)$_2$CH$_3$
84: R$_1$ = Ph

78: R$_1$ = CH$_2$CH$_3$ (73%)
79: R$_1$ = (CH$_2$)$_2$CH$_3$ (63%)
80: R$_1$ = Ph (100%)

85: R$_1$ = CH$_2$CH$_3$ (100%)
86: R$_1$ = (CH$_2$)$_2$CH$_3$ (100%)
87: R$_1$ = Ph (82%)

49: R = 2-CH$_3$
77: R = 4-F

H$_2$SO$_4$, rt, 72 h

32: R$_1$ = CH$_2$CH$_3$; R$_2$= 2-CH$_3$ (43%)
33: R$_1$= (CH$_2$)$_2$CH$_3$; R$_2$ = 4-F (16%)
34: R$_1$=Ph; R$_2$ = 4-F (10%)
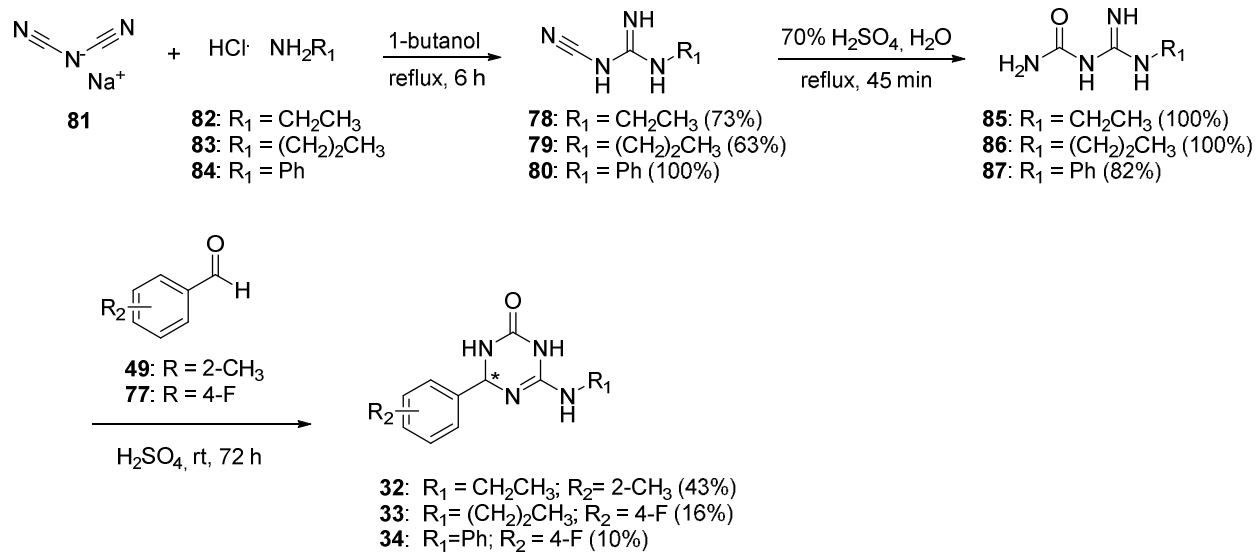
Scheme 4. Synthesis of 6-alkyl/-arylamino-4-aryl-3,4-dihydro-1,3,5-triazin-2(1*H*)-ones **32-34**.

TABLE OF CONTENTS GRAPHIC